INTEFERENCE OF TONIC MUSCLE ACIVITY ON THE SCALP RECORDED EEG SIGNAL

by

Gizem Yılmaz

A Thesis Submitted to the
Graduate School of Health Sciences
in Partial Fulfillment of the Requirements for
the Degree of

Master of Science
in
Medical Physiology

Koc University

August 2014

Koc University

Graduate School of Health Sciences

This is to certify that I have examined this copy of a master's thesis by

Gizem Yılmaz

and have found that it is complete and satisfactory in all respects,
and that any and all revisions required by the final
examining committee have been made.

Committee Members:

Prof. Dr. Kemal S. Türker (Advisor)

Prof. Dr. Bayram Yılmaz

.

Doç. Dr. Bahar Güntekin

Date: 20. 08.14

ABSTRACT

Electroencephalography (EEG) is an important tool for the measurement and monitoring the brain's electrical activity. EEG signal is recorded with electrodes placed on the scalp. However, the electrical activity of muscles can interfere with the electroencephalogram (EEG) signal considering the anatomical locations of facial or masticatory muscles surrounding the skull. Temporalis muscle (*m. temporalis*) holds the mandible in physiological rest position and it covers a large area under the EEG electrodes. In this study, we evaluated the possible interference of the resting activity of the temporalis muscle on the EEG under conventional EEG recording conditions. In 9 healthy adults EEG activity from 19 scalp locations and single motor unit (SMU) activity from anterior temporalis muscle were recorded in three relaxed conditions; eyes open, eyes closed, jaw dropped. For the analysis of the data, EEG signal was spike triggered averaged (STA) for different EEG electrode locations. Action potentials of SMUs were used as triggers for the STA procedure. Resting temporalis SMU activity generated prominent Macro-EMEG (electro-myo-encephalogram) potentials with different amplitudes, reaching maxima in the proximity of the recorded SMU. Interference was also notable at the scalp sites that are relatively far from the recorded SMU and even at the contralateral locations. The head and neck are surrounded by muscles with a great number of SMUs. Therefore, EEG is highly susceptible to muscle activity artifacts even under rest conditions. This study emphasizes the need for efficient artifact evaluation methods which can handle muscle interferences.

ÖZET

Elektroensefalografi (EEG), beynin elektriksel aktivitesi ve fonksiyonlarının takibinde başvurulan temel yöntemlerden birisidir. Kafatasını çevreleyen saçlı deri üzerine yerleştirilen elektrotlar aracılığıyla EEG sinyali kaydedilir. Ancak, çiğneme ve mimik kaslarının anatomik yerleşimleri göz önüne alındığında, EEG sinyali kasların elektrik aktivitesinden kaynaklanan Elektromiyografi (EMG) sinyali ile karışmaktadır. Temporal kas (*m. temporalis*) mandibulayı dinlenme pozisyonunda tutan kastır ve EEG elektrotları altında geniş bir yüzeyi kaplamaktadır. Yaptığımız bu çalışmada, dinlenme durumundaki temporalis aktivitesinin EEG sinyaline olan karışımı/kontaminasyonu incelenmiştir. Dokuz sağlıklı ve yetişkin gönüllüde, 19 elektrot yerleşimli EEG sinyali ve anterior temporalis Single Motor Unit (SMU) aktivitesi, 3 farklı koşulda (gözler açık, gözler kapalı, çene düşük) eşzamanlı olarak kaydedilmiştir. EEG sinyali, her bir SMU aksiyon potansiyelinin trigger olarak alınmasıyla Spike Trigger Average (STA) yöntemi ile analiz edilmiş ve SMU aktivitesinin farklı EEG elektrotlarına nasıl yansıdığı değerlendirilmiştir. Dinlenme durumundaki temporalis aktivitesi EEG sinyalinde belirgin Macro-electro-myo-encephalogram (Macro-EMEG) potansiyelleri oluşturmuştur. Oluşan Macro-EMEG'lerin genlikleri farklı olup kaydedilen SMU yakınında maksimum değerdedir. EEG sinyaline olan karışma, kaydedilen SMU'dan görece uzak olan kısımlarda ve kontralateral tarafta da gözlenmiştir. Baş ve boyun kaslarında mevcut SMU sayısı göz önüne alındığında, aktif kasılma olmadığı durumda dahi tek bir motor ünitenin EEG sinyalini kontamine edebilmesi, EEG sinyalinin kas aktivitesine olan hassasiyetini açıkça göstermektedir. Bu çalışma, kas aktivitesinden kaynaklanan elektriksel sinyalin EEG'ye karışımını önlemede kullanılabilecek etkili yöntem ve metotların gerekliliğine dikkat çekmektedir.

ACKNOWLEDGEMENTS

I would like to express my deepest gratitude to my advisor, Prof. Kemal S. Türker, for his excellent guidance, caring, patience, and providing me with an excellent atmosphere for doing research. I would like to thank Prof. Pekcan Ungan, Dr. Oğuz Sebik and Dr. Paulius Ugincius for their valuable help in the research and their support.

I would also like to thank my parents and my brother. They were always supporting me and encouraging me with their best wishes.

TABLE OF CONTENTS

Chapter 3: Temporalis activity at rest

Chapter 4: Methods

Chapter 5: Results

Chapter 6: Discussion

LIST OF TABLES

LIST OF FIGURES

PREFACE

The motive of the study we introduce in the following chapters historically stems from a profound discovery of the 19th century: electricity of the living tissues. The observations of Galvani (1737-1798), Volta (1755-1832), Ohm (1787-1854) and Faraday (1791-1867) about the electricity paved the way for the first muscle-electricity preparations. For the first time, Matteucci (1811-1868) observed the action potential during the contraction of frog muscle. [1] Du Bois-Reymond (1818-1896) introduced the term "muscular current" and developed none-polarizable electrodes made of clay which were used in animal and human EEG recordings for many years (as cited in [2]). Bernstein (1838-1937) established the membrane theory of ionic action currents. [2]. The advancements of the electricity measurement tools such as galvanometers and electrometers continued during the 20th century. By this time, physiologist started to experiment on animals and to measure the electricity of living tissues using these tools. Caton (1842-1926) recorded the electrical activity from the brains of rabbits, cats and monkeys using the non-polarizable electrodes. Berger (1873-1941) followed the implementations of Caton's early EEG studies [3]. Furthermore, he used, modified and developed the existing electrophysiological measurement devices until he was able to make a recording of human EEG. Today, we are using "alpha" and "beta wave" terms essentially as he established. The burst of experimental and clinical EEG studies in Europe and America continued with the commercialization of the EEG instruments by the mid 1930s [2]. As the EEG instruments became more sophisticated, the understanding of the brain activity progressed. Today's computerized EEG systems enable researches to record with high sensitivity, to store huge amount of data and to analyze precisely. However, the signal recorded with the EEG devices still does not represent exact brain activity. Our hypotheses in this study basically deals with the controversial question of "what makes the EEG".

CHAPTER 1

MUSCLE ARTIFACTS IN THE EEG

The electroencephalogram (EEG) has been used widely to diagnose, monitor and evaluate neurological states in clinics. As a non-invasive screening tool for the neuronal functions, the EEG gained a historically important role in the neuroscience clinics and in the experimental studies. From the cognitive problems to the structural defects, many researchers start investigating by looking at the EEG records. However, measuring a cerebral activity from the scalp surface gives rise to a question about the interfering signals and/or artifacts. Before starting to discuss the EEG-EMG problem, we should have a brief look at these electrophysiological measurement tools and signal properties.

1.1 Generation of the EEG signal

Electroencephalography (EEG) is a measurement tool of the cerebral electrical activity. However, the EEG represents not directly the electrical activity of neurons but the current dipoles produced by the synaptic events. The activity of neurons in the brain produces some magnetic fields and volume conducted electrical currents which are recorded as the EEG signal [4].

The main source of the scalp recorded EEG is not the propagating action potential (AP) but the extracellular flow of currents due to the excitatory or inhibitory synaptic events between cortical cells. Based on the type of the neurotransmitter and receptor, synapses can be excitatory or inhibitory. If an action potential (AP) travels along the fiber which ends in an excitatory synapse, an excitatory postsynaptic potential (EPSP) occurs in the following neuron. Summation of EPSPs triggers an AP on the postsynaptic neuron. If an AP travelling along the fiber ends in an inhibitory synapse, inhibitory postsynaptic potential (IPSP) occurs due to hyperpolarization [5].

Pyramidal cells are the main generators of the EEG. They are ordered in a histoanatomical arrangement with the stellate cells. While the stellate dendrites are branching spherically, the conically shaped pyramidal neuron always faces the cortical surface with the apex and they have very long apical dendrites.(Fig 1.1) This histoanatomical arrangement of the pyramidal cells provides layers of current dipoles which enables to record the synchronized activity which we record as the EEG [4].

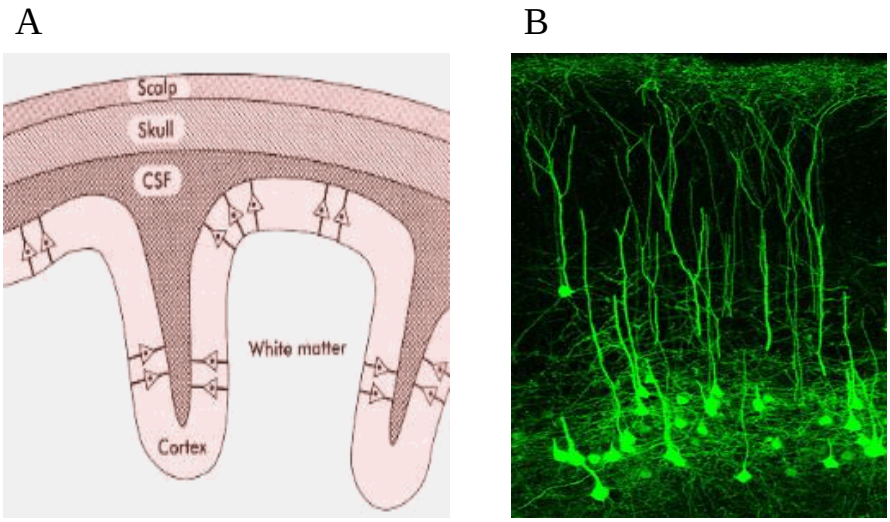

Fig. 1.1: **Histoanatomical arrangement of pyramidal cells**. **A**.Vertical arrangement of the pyramidal cells and dendrites from a cross-sectional view of the head. The postsynaptic potentials pass through the membranes surrounding the brain, CSF (cerebrospinal fluid), continue on up through the skull to appear finally at the scalp as recorded as the EEG. (depicted from[6]). **B** The brain section of the somatosensory cortical area pyramidal neurons and their dendrites (depicted from [7]).

Electrical field generated by the ionic current flow is modeled as current dipoles (Fig 1.2). When an excitatory synaptic input arrives to the dendrite of the pyramidal neuron, intracellular current flows from less negativity to more negativity. Extracellular current flows back from the soma to the dendrite which is represented as an extracellular current dipole. If the soma of neuron is excited, the intracellular current flows to the dendrite while generating an extracellular current dipole from dendrite to soma [4, 8].

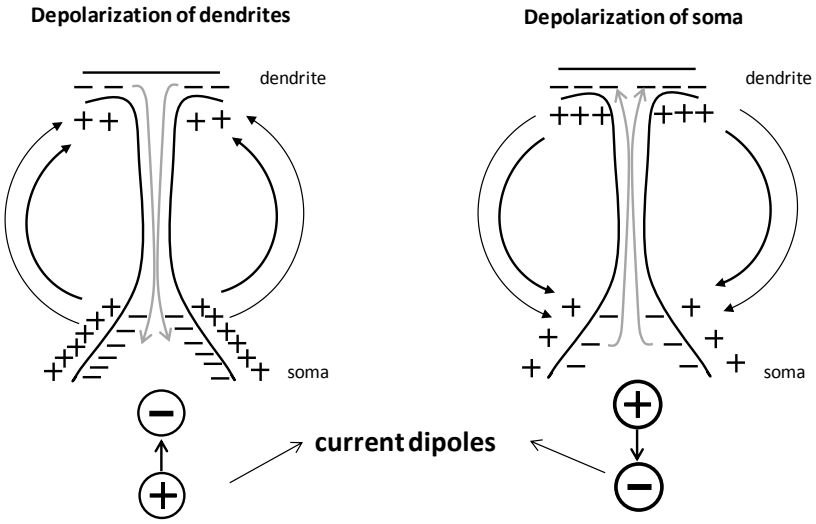

Fig 1.2: **Current dipole formation.** Depolarization of dendrites causes extracellular current to flow back from the soma to the dendrite. Depolarization of soma results in an extracellular current dipole from dendrite to soma (Depicted from[4]).

Direction of the current dipole either from dendrite to soma or the reverse determines the polarity of the EEG signal. Fig 1.3 illustrates the effect of dipole direction on the polarity of the surface recorded signal. An excitatory input to dendrite leads to a negative polarity in the extracellular space. Positive charges travel within the apical dendrite, and they evoke an extracellular positivity at the soma. A negative dipole is generated and displaced with an upward deflection at the scalp (Fig 1.3 A). An excitatory input to soma causes a negative polarity in the extracellular space. Positive charges spread within the apical dendrite, and they generate an extracellular positivity at the dendrite. A positive dipole is produced and displayed with a downward deflection at the scalp (Fig 1.3 B) [8].

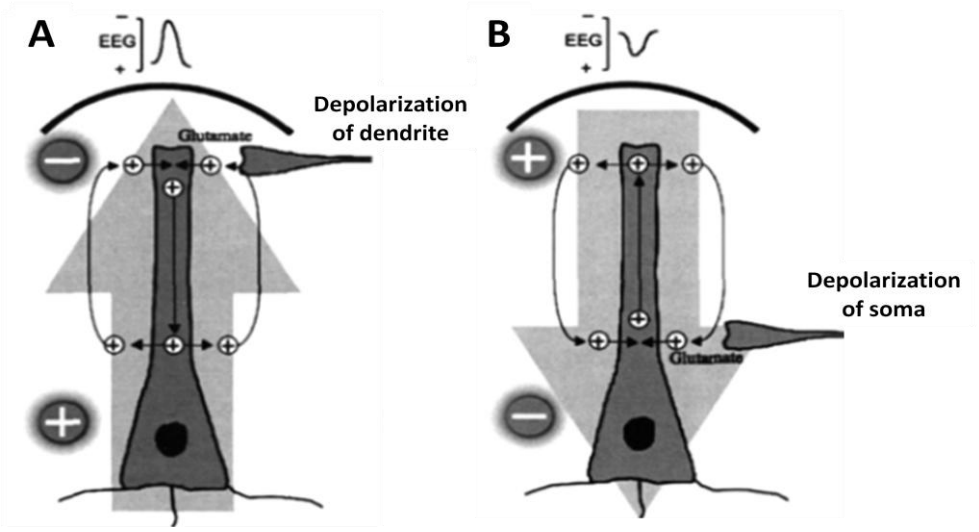

Fig 1.3: Polarity of the EEG signal. The EEG electrodes record potentials for dendritic depolarization as a surface-negative (upward) (**A**) and for somatic depolarization as a surface-positive (downward) (**B**) (Depicted and modified from [8])

Cortical pyramidal neurons are excellent dipoles due to their unique anatomical structure with a long apical dendrite perpendicular to the cortical surface. Hence, the EEG is the total of all excitatory and inhibitory postsynaptic potentials of cortical pyramidal neurons that produce a vertical dipole perpendicular to the scalp [4].

The generated dipoles spread through the various tissues with different conductivities, the brain tissue, the skull and the skin covered scalp, respectively until they reach to the EEG electrode due to volume conduction (Fig 1.4). However, the volume conduction makes the signal vulnerable to the several types of artifacts [9]. It is possible to have direct measurements of brain activity using intracranial EEG (iEEG) electrodes which are crucial in

the assessment of patients with epilepsy [10]. As being an invasive measurement tool, the iEEG is subject to several discussions about the dangers [11]. However, the scalp EEG is a noninvasive monitoring tool for the daily clinical use or the sophisticated brain computer interface systems, hence, recognition and the handling of artifacts in the scalp EEG have gained much more importance in recent years.

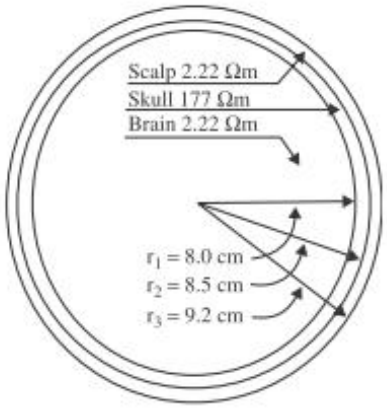

Fig 1.4: Conductivities of the three main layers of the brain: brain, skull and scalp. Approximate thickness (r) and resistivity (Ωm) (Depicted from [3].

1.2. Generation of the EMG signal

A motor neuron innervates several muscle fibers within a striated muscle. The motor neuron and the muscle fibers innervated by this motor neuron compose a functional unit of striated muscle contraction which is defined as the Motor Unit [1]. Motor Unit (MU) is the smallest muscular unit which consists of a single alpha motoneuron with its long axons and terminal branches, its neuromuscular junction and the muscle fibers it innervates (from few to thousands) (Fig 1.5)

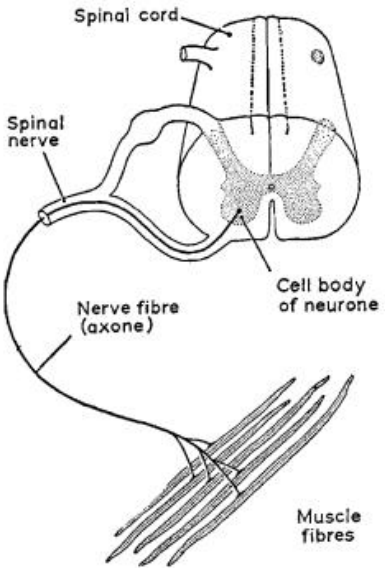

Fig 1.5: Scheme of a Motor Unit. Axons of motor neurons extend from the spinal cord to the muscle. There, the axon divides into a number of axon terminals that form neuromuscular junctions with muscle fibers scattered throughout the muscle (Depicted from[1])

A single action potential propagating down the motor neuron activates all the muscle fibers in the motor unit. All the muscle fibers in one MU contract simultaneously by an impulse descending from the motor neuron. Hence, activation results in the depolarization of the muscle fiber membrane which generates an electromagnetic field due to the movements of ions through the membrane. But, the activation of different muscle fibers of the same MU does not occur synchronously. First, the length and diameter of the individual axon branches innervating individual muscle fiber vary and introduce a delay.This delay is fixed for each muscle fiber. Second reason of the delay is the random discharge of acetylcholine released at each neuromuscular junction.Therefore, the excitation of each muscle fiber is a random function of time [1].

An electrode that is placed in the vicinity of the muscle fiber records the voltage respect to ground (Fig 1.6). The voltage change in time is the representation of a single action potential [12].

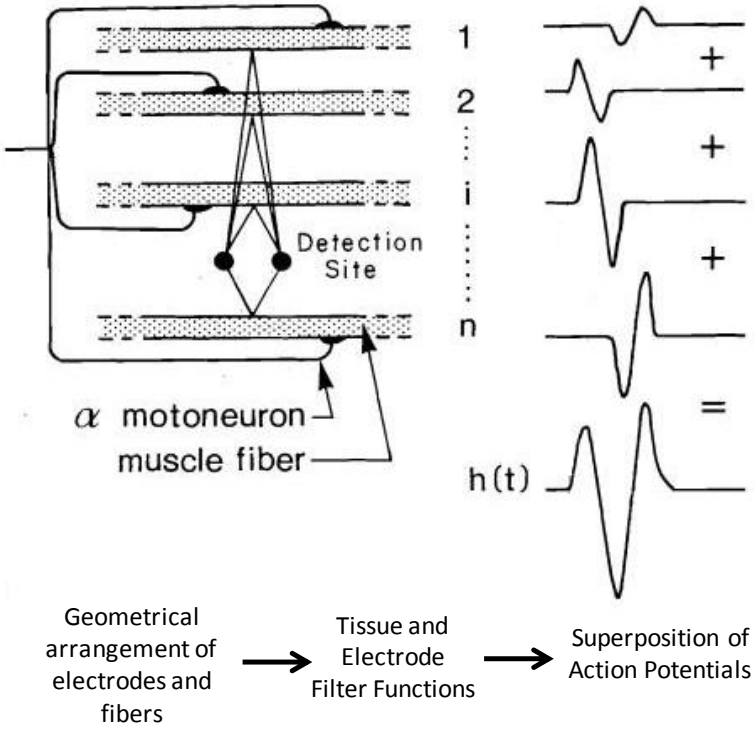

Fig 1.6: **Generation of the motor unit action potentials (MUAPs)** (Depicted from [13])

Individual action potentials belonging to the muscle fibers of a motor unit overlap in time. The recorded motor unit action potential (MUAP) represents a spatial-temporal overlapping of the separate action potentials. H(t) in Fig 1.6 depicts the resultant triphasic MUAP signal of the muscle fiber depolarization [13]. The shape and the amplitude of the MUAPs are affected by the positioning of the electrodes relative to the fibers and the tissue layer between the fibers and the detection site. Fig 1.7 illustrates the decomposition of the EMG signal into MUAP constituents which recorded over time [12]. Consequently, the signal recorded from the surface of the skin, namely the surface electromyogram, is the summation of the distinct MUAPs whose duration and amplitude change due to tissue filtering [13].

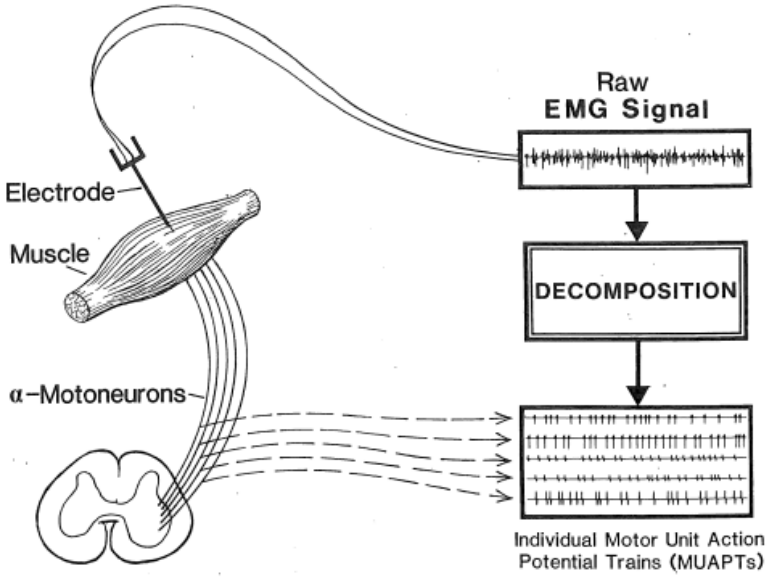

Fig 1.7: **Decomposition of the EMG signal into MUAP trains** (Depicted from [12])

Conventionally, the surface EMG (s-EMG) and the intramuscular EMG (i-EMG) are used for indirect measurement of the nervous system. The s-EMG is able to record the activity from large and superficial muscles and it is susceptible to the changes in the skin resistance [14]. By inserting a needle or wire electrodes into the muscle, it is possible to record from the single or few muscle fibers [15]. For the monitoring of deep and small muscles, thei-EMG is preferred. Hence, the area to be recorded can be determined by adjusting the length of active tip of the wire and the recording is not affected from the skin resistance [14]. Therefore, both methods are valuable for the researchers who study functional anatomy of muscles, excitability of motoneurones, biofeedback, muscle force and the reflex pathways [15].

Consequently, the action potentials are the main generators of the EMG, however, the EEG represents the postsynaptic activities between neurons not the action potential itself. The EMG differs from the EEG in terms of the origin of the signal.

1.3. Artifacts in the EEG

Artifacts are undesired signals that can involve in the recorded brain signal and mislead the EEG researchers during the interpretation of the data.

Artifacts have either non-physiological sources (such as 50/60 Hz power-line noise, changes in electrode-skin impedances, etc.) or physiological/biological sources [9].

1.3.1. Biological Artifacts

Biological artifacts arise from the subject's / patient's physiological activites and spread across the body from source to the recording area. The most common biological artifacts are the muscle activities, movements of eyes, respiration and the beating of heart [16].

The relatively high cardiac electrical potentials propagate through the body and interfere with the EEG signal [17, 18]. Electrocardiogram (ECG) peaks might appear in the EEG signal with various amplitudes. Small cardiac related movements of the body, movements of arteries around the scalp between systole and diastole and the voltage changes due to the speed change of blood in the arteries cause ECG artifacts [19].

Eye movements which include eye blinks, eye movements (such as rolling) and saccades constitute one of the major biological artifacts because voltage field generated by the eye movements distort the original EEG signal. The movement of the eye or the movement of the eyelid might cause the interference [20]. It is comparatively easy to recognize and to extract high amplitude eye blink artifacts from the EEG recording.

However, because of the high amplitude of eye blink, it has a significant effect on the results of the EEG analysis. The eye blink possibly disturbs the evoked potential in event-related-potential (ERP) studies. Hence, the act of blinking has a direct relation to the mental states like drowsiness [21]. On the other hand, the small-amplitude eye movements and the myogenic signal arising from ocular muscles have an important influence on the EEG and several authors indicated the risk of interpreting ocular muscle activity as a cortical response [22, 23].

Therefore, myogenic artifacts constituted one of the major problems in the EEG interpretation. Many studies have reported that the electromyogram (EMG) signal originating from facial or masticatory muscles can contaminate the EEG [16, 24-30].

1.4. Myogenic artifacts as a challenging problem

While recording the EEG, the subjects sit or lie down, relax and only attend to the signs/ suggestions that appear on a monitor. Subject can passively read a book/ watch a muted film with subtitles to make her/him ignore any stimulus and avoid drowsiness.

Normally, movement of head, body, jaw or tongue generates disturbances with high amplitudes which are quite easy to recognize and to extract from the EEG signal [16]. However, under relaxed recording conditions, many facial, mimic and masticatory muscles are unintentionally activated to keep the head up [31, 32], the mouth closed [33, 34], the eyes open and the facial gesture expressed [35- 37]. Therefore, it is not possible to silence muscles for the ease of recording and the interference of this unintentional muscular activity with the EEG signal may go unnoticed.

On the other hand, to illustrate the interference between the EMG and the EEG signals, researchers asked subjects to voluntarily contract their (facial or masticatory) muscles during the EEG recording sessions [24, 26, 27, 38, 39]. Muscle interference was evaluated between the periods of relaxation and muscle contraction. The reported degree of contamination as a result of contraction was not surprising due to the volume conduction and the crosstalk from the neighboring muscles / sources of bioelectrical potentials [40] considering the anatomical proximity of muscles over the scalp.

1.5. Nature of the problem

1.5.1.Frequency overlap

Cortical neurons display various synchronization patterns in different consciousness stages. The frequency of the EEG ranges between the ultra slow and ultra fast frequency components. However, clinically important frequency range is broadly accepted between 0.1 Hz and 100Hz, in a more restricted sense, from 0.3Hz to 70 Hz [41]. The EEG frequency range is broken down into frequency bands which have functional importance in the clinics. **Delta** band contains frequencies below 3.5 Hz (usually 0.1-3.5/sec). **Theta** is between 4 and 7.5 Hz, **Alpha** is 8-13 Hz and **Beta** is 14-30 Hz. **Gamma** band covers the frequencies above 30 Hz [41]. Each of these bands has functional links to the cognition and the physiology of brain.

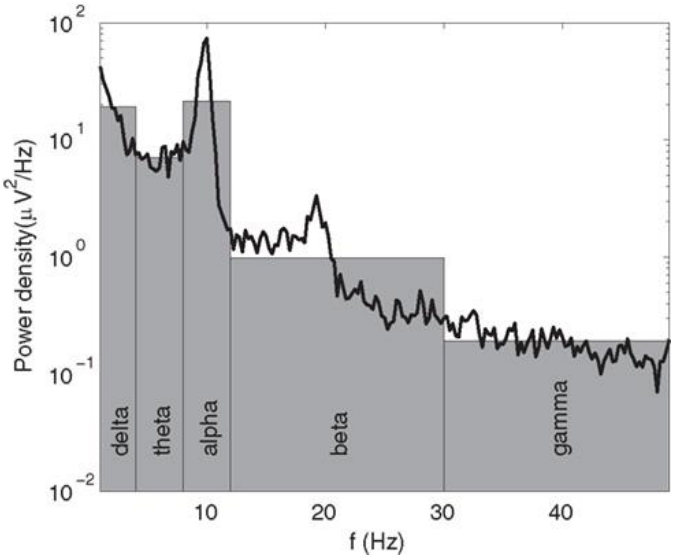

Fig 1.8: EEG frequency bands. Schematic representation of the EEG spectrum with band powers of each band (Depicted from [42])

On the other hand, the power spectrum of the striated muscle activity lies between 20-500 Hz when measured with surface EMG [14]. Lower end of this frequency range contains the most of the power of the EMG [15]. Consequently, the main reason for the muscular contamination is the broad overlap between the EEG and the EMG power spectra. The alpha (8-13 Hz), beta (14-30 Hz), and particularly gamma (above 30 Hz) bands showed contamination by activity of different scalp muscles [23, 26, 27, 38, 44, 45].

1.5.2. Topography of myogenic artifacts

Due to the anatomical placement of the corrugator, orbicularis oculi, frontalis, masseter, temporalis, occipitalis and the peri-auricular muscles (Fig 1.9) –almost all head muscles- might interfere with the EEG signal [46].

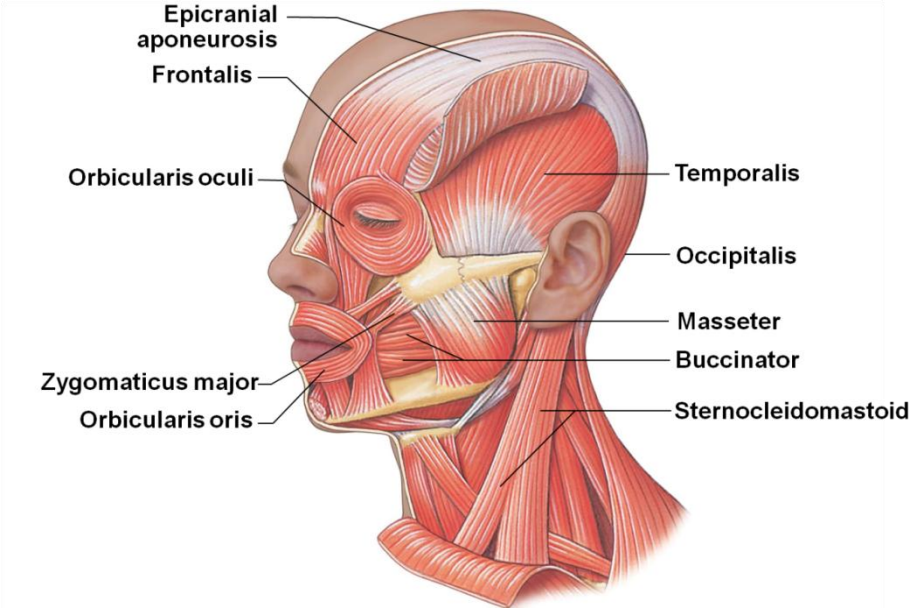

Fig 1.9: **Lateral view of head muscles** (Depicted from[47])

Temporalis and Frontalis

The activity of the temporalis and the frontalis muscle affected frontal, temporal and central EEG leads in previous studies [26, 27, 39, 46]. The power spectra of frontalis muscle showed a main peak at around 30 Hz [26, 27] during voluntary eyebrow raising. Similarly, the power spectra of temporalis muscle presented two broad peaks during teeth clenching around 20 Hz and between 40-80 Hz [26, 27]. Hence, even weak contraction of frontalis and temporalis muscle affected the EEG spectra significantly depending on the strength of muscle activity. Temporalis and frontalis muscles exhibited low level of EMG even in the supine rest position [48]. Also, recent paralysis studies confirmed the effect of temporalis and frontalis muscle activities on the EEG, especially on gamma band (30Hz and above frequencies) [29, 49]. Whitham and colleagues (2007) reported that the high frequency power which was evident around temporal-frontal muscles in resting unparalysed state declined significantly after paralysis in the frequencies above 20-30 Hz.

Ocular muscles

The myogenic signal arising from ocular muscles interfere with cortical gamma band response [22, 23, 45]. The EMG activity of ocular muscle manifests a saccadic spike (SP) potential which produces a high frequency activity with a peak around 65 Hz [45]. Saccadic

spikes are observed at the onset of even tiny saccadic eye movements and they reflect the engagement of the extraocular muscles in the orbit [22]. The power spectra of these saccadic potentials showed a broadband peak in the gamma band from 32 Hz to 128 Hz [45] which overlap the cortical gamma band activity at the frontal and the posterior electrodes. Since the neuronal gamma band (above 30 Hz up to 100 Hz or above) activity is considered centrally important for cognitive functions [50], muscle artifacts constitute a serious problem especially for visual and/or mental task dependent EEG studies [51].

Neck muscles

Activity of posterior head muscles also creates artifacts in the EEG. Kumar *et al.* (2003) reported that the EMG activity of sternocleidomastoids, splenus capitis and upper trapezius shows a power spectra peak between 80 Hz and 120 Hz during voluntary contraction from rest to maximal which might coincide with the high gamma activity. Paralysis studies showed a decline in the high frequency power around cervical muscles after paralysis [29]. It was indicated that the tension might be generated in the neck muscle – splenus capitus - as a result of motivational modulation [52]. Relation between motivational situation and tension gained a big importance as muscle tension in corrugator and frontalis were found increased as a result of an increase in auditory and mental task difficulty [53]. It is clear that subject's emotional stress and attentional situation might have a direct effect on the myogenic artifact contribution to the EEG.

Auricular muscle

Another interesting muscle artifact was been reported by Meulen *et al.* (2006) where a muscle artifact from the posterior auricular muscle (behind the right ear) was introduced [54]. Spectral analysis of the posterior auricular muscle showed frequency range between 20 Hz and 30 Hz. The posterior auricular muscles can be activated even by swallowing and breathing.

It is very important to note that the EMG activity of facial-head muscles shows a considerable spectral variability in amplitude, peak frequency and band width. Factors such as active muscles, contraction strength, location and lateralization might also affect the outcome – the EEG.

CHAPTER 2

CURRENT METHODS FOR THE HANDLING OF THE EMG ARTIFACTS

Fatourechi *et al*. (2007) reported that only 3,2 % of more than 250 papers used removal algorithms for muscle artifacts such as linear filtering, regression and component based algortihms [16]. Due to the broad overlap on the frequency bands of the EEG and the EMG, it is very crucial to handle muscle artifacts without losing the information of interest in the signal. For this reason, there is a great effort in developing computer based algorithms and "clever" detection methods to produce an "artifact free EEG".

2.1. Filtering

Filters are components placed in the amplifier and they process the signal to eliminate unwanted (higher or lower) frequencies. Each filter has a frequency range which it can eliminate without distorting the original signal. The high frequency filter attenuates high frequencies in amplitude, so it is also called as a **low-pass filter**. Likewise, low frequency filters which is known as **high-pass filters** attenuate the low frequencies below a specific frequency and allow higher frequencies without distortion [4].

Conventional EEG filters, which are mostly set to 0.1 Hz high pass and 70 Hz low pass [41] are insufficient to reduce the EMG interference because it is known that the EEG and the EMG spectra overlap in a broad frequency range. Hence, filtering methods have gained much criticism and interest [55]. Therefore the conventional filtering methods are being replaced with several other artifact removal methods such as spatial filtering [49, 55], adaptive filtering [56]and component based algorithms such as Independent Component Analysis (ICA) [57, 58], Principal Component Analysis (PCA) or Canonical Component Analysis (CCA) [59].

2.1.1. Spatial filtering

The ear reference (right or left), monopolar montage, bipolar montages, the Common Average Reference (CAR) and the Laplacian Derivation are the most commonly used spatial filters. The ipsilateral ear reference (right or left ear) or the vertex reference (Cz) montages are common in the EEG laboratories.

However, due to the location and the orientation of the source, selected montage might be misleading if it is not relatively inactive [60]. If the selected reference is active or close to the active source, the montage itself might create distortion in the true amplitude and waveform of the signal. In the case of muscle artifacts, reference may interfere as an artifact if the reference is above the active muscle.

Location and the extent of the control signal and artifacts determine the proper spatial filter selection that should provide the highest signal-to noise ratio (SNR) [55]. Among commonly used spatial filtering methods, Laplacian filtering eliminated muscle artifacts in a more sensitive manner [26, 39, 55]. Basically the Laplacian method uses the second derivative of voltage distribution of each electrode location and thereby it emphasizes higly localized activity and reduces more diffuse activity [61]. The Common Average Reference (CAR) subtracts the average value of the entire electrode montage (the common average) from the EEG channels and components is accentuated with highly focal distributions. However the precision of CAR decreases with the decrease in the electrode placement density [61, 62]. Even though spatial filters function as a high pass filter, the sources they accentuate show different distributional characteristics; hence they can not remove the muscle artifacts.

2.1.2. Adoptive filtering

Adoptive filtering is a combination of the spatial filtering and the frequency filtering [56]. Recently this technique has been evaluated for removing muscle artifacts [56, 63].

2.2. Coherence

Coherence analysis, cross correlation and cross spectral density analyses were used to asses inter-electrode relationships and variance in the EEG [24, 38, 64, 65].

Coherence is a measure for quantifying the linear correlation between two signals in the frequency domain and provides both amplitude and phase information of two related oscillatory signals at a particular frequency [66]. If two signals have a consistent relationship between their phases (phase coherence) or power (spectral coherence) over time with a zero phase difference (zero lag), they are considered as coherent or synchronised or phase locked [67]. Coherence provides a normative measure of the strength of association on a scale from 0 to 1, with 1 indicating a perfect linear relationship and zero occuring in the case of independence [68].

To find out synchronous activities through cortico-muscular system, EEG is correlated spectrally with sEMG recordings during a specific task. Halliday et al. (1998) revealed a correlation in 15-30 Hz range - which is called β rhythm - between EEG recordings over sensorimotor cortex and sEMG of limb muscles during voluntary contraction performances [69] Both of the EEG and EMG showed the same rhythmical activity in 16-36 Hz. β band (15-30 Hz) corticomuscular coherence is known to be most prominent during steady contractions while being abolished by movement [66]. β coherence was assumed to be responsible in maintaining a stable motor output with a minimum effort [70].

O'Donnel *et al*. 1974 investigated the coherence between the EEG and the temporalis and masseter muscles [24]. The coherence increased significantly with the muscle contraction above 14 Hz. But especially in frequencies below 20 Hz, coherence analysis was not affective in addressing the possible nonlinear interactions Srinivasan *et al*. (1998) observed distinct patterns of source correlations at 10Hz and the coherence declined at high frequencies (above 38Hz) [65]. The high frequency activities (above 30 Hz) were spread more easily due to volume conduction confirming the inefficiency of the filtering and coherence methods. Even tough the EEG coherence is the result of neocortical source activity, signal should pass through the tissues of head and the scalp EEG is spatially low-pass filtered by the poorly conducting skull. Therefore, volume conduction introduces artificial correlation between the electrodes [65].

2.3. Component Based Algorithms

Main assumption of component based method (such as Independent Component Analysis (ICA), Principal Component Analysis (PCA), Canonical Correlation Analysis (CCA) is that the EEG is an output of a number of statistically independent brain processes [71]. Consequently, a multichannel EEG data can be decomposed into signal components (sources) by using a decomposition algorithm.

ICA is one of the widely used artifact removal methods in literature [57, 58, 71, 72]. Basically, the ICA blindly separates the EEG into temporally independent sources of activity [57]. Each datum recorded from an electrode is projected on a vector and these vectors form the independent components space. Intuitively, by assessing the statistical properties of the data in this space, artifacts are isolated and removed [72].

PCA is another method that is used removal of muscle artifacts [59, 73]. The PCA creates a covariance matrix of EEG signal and finds the projection of the data with greater variances [73]. The PCA has been mostly recommended for removing low frequency ocular artifacts. For both ICA and PCA, once the independent time courses of different brain and artifact sources are extracted from the data, "corrected" EEG signals can be derived. However Jung *et al.* (2000) claimed that the ICA is more advantageous than the PCA in detecting artifacts because the PCA can find orthogonal directions of variance but neurological EEG sources can be nonorthogonal [57]. The effectiveness of the PCA in segregating sources also was lower than the ICA [73]. On the other hand, the effectiveness of the ICA in removing EMG from data is debated because (1) neurological expertise is needed to decide which sources are artifacts, (2) manual identification is time consuming, (3) removal of determined artifacts can cause a loss of neurological signal, (4) cleaned EEG still can contain muscle artifacts [46, 58, 74].

CCA is a more recent source separation technique. The CCA outperformed the ICA in removing muscle artifacts from the EEG [59, 75]. The CCA measures the linear relationship between two dimensional random variables by using second order statistics [76]. Especially the CCA was used in combinations with other algorithms such as the ICA to increase the effectiveness [59, 76, 77].

Another source separation based method is Wavelet Transform (WT) which was suggested recently to remove myogenic artifacts from the EEG [77]. Wavelet transform or denoising simply performs blind source separation and transforms data to wavelet domain composed of several frequencies. Then it extracts sources from the signal by applying a threshold [78]. However, for low signal to noise ratio signals, the WT was found weak [77].

Ideally any of these validation and removal techniques should posses a high degree of sensitivity and specificity which means that while attenuating muscle artifacts, electroencephalographic signals must be preserved. But, a best method to remove all kind of muscle artifacts without losing informative EEG signal is absent for now.

CHAPTER 3

TEMPORALIS ACTIVITY AT REST

3.1. Properties of the temporalis muscle

The temporalis muscle is one of the muscles of mastication. Masticatory muscles produce the jaw movement and the force applied by teeth and temporomandibular joints [79]. The movement of human mandible is guided by the two temporomandibular joints through mastitory muscle activity.

The masticatory muscles are grouped as elevators and depressors. The elevator group consists of the masseter, temporalis and medial pterygoid muscles and the depressor group contains geniohyoid, mylohyoid, digastrics and lateral pterygoid muscles [80]. The elevator muscles have dense pennations and large cross-sectional areas to generate high forces [79]. However, the depressors are suitable to contract over long distances with less force.

Temporalis muscle functions as a jaw elevator. Anatomically, temporalis is a fan shaped muscle whose long fibers (17 to 54 mm, average 34 mm) originate from the temporal fossa and ends at the coronoid process and the anterior border of the ascending ramus [79]. Fig 3.1 illustrates the temporalis muscle.

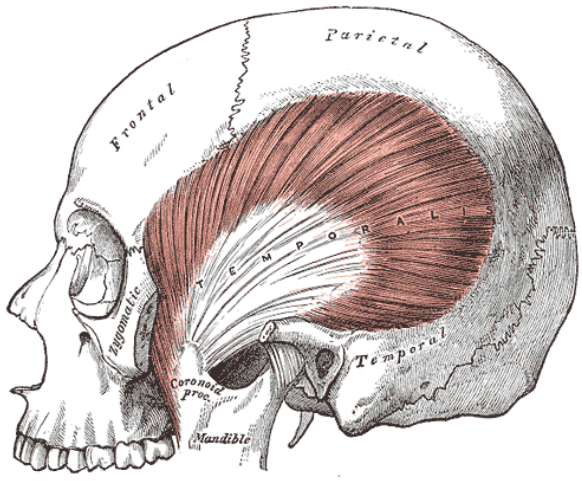

Fig 3.1 : **Temporalis muscle** (Depicted from [81])

Anterior part of temporalis has the largest cross sectional area [79] and its role in regulating mandibular posture was questioned [82- 85]. Mandible is kept in a stable position relative to the maxilla (2-3 mm between the upper and lower incisors) in physiological rest position [86]. Temporalis muscle as the largest elevator of the mandible [87] was claimed to be responsible for the mandibular rest position [33, 87- 89].

Dense spindle population of temporalis [90] and predominance of type I fibers among type IIA, IIX and hybrids [91] indicate the role of anterior part in tonic activities. During actions of jaw elevation such as biting, chewing and jaw closing, the intensity of work is higher for the anterior portion than the posterior. Fiber type distribution studies revealed the large number of type I muscle fibers in the anterior part [82, 91]. Type I fibres are activated first [92], and their innervations ratio is small. The structure of the temporalis muscle enables the anterior muscle portions to regulate the magnitude of the produced chewing or biting force in a precise manner.

3.2. New approach: Recording of the temporalis SMU activity

For a long time, the EEG recorded at rest was assumed to contain a very low level of muscle artifact [25] or ignored [27, 44]. Muscle interference at rest is a relatively recent concept. Goncharova and his colleagues (2003) revealed the presence of considerable interference from the pericranial muscles to the EEG in the experimental rest position [26]. Later on, paralysis studies confirmed the EMG contamination of EEG [29, 49, 93]. The muscle activity diminished with the injection of curarizing agent.

The use of surface EMG was the common approach among EEG studies to date [24, 26, 27, 29, 39, 49]. Either the EMG electrodes attached on the facial muscles or the EEG electrodes measured the EMG activity from the surface of the skin. However, the limitation of SEMG becomes more evident while measuring the resting activity of face musculature because of the crass-talk phenomenon.

The SEMG is susceptible to the crosstalk from the neighboring muscles [40]. Electrodes/sensors placed on the skin detect the activity of target muscle as well as the volume-conducted EMG signal from neighbouring muscles because the electrodes record the tissue filtered electrical activity of concurrently active motor units in a volume conductor [94]. The anisotropic nature or the nonhomogenity of muscles lead to cross-talk. The surface EMG may lead researchers to the faulty evaluation of the muscle artifacts due to the cross-talk

and the frequency overlap. Amplitude of the cross-talk signal might be as great as 16 % of the stimulated muscle signal [94].

However, intramuscular electrodes are able to detect the activity of small or deeply located muscles [14]. Using intramuscular wire electrodes, the activity of a single muscle fiber (single motor unit) or of the several fibers (multi motor unit) can be recorded. Hence, the action potential is an all or none event and the motor unit potentials represent only the activity of the muscle of interest. The intramuscular wire EMG is more advantageous than the surface EMG since the cross-talk does not interfere with the recorded muscle activity, namely single motor unit potentials [14]. Therefore, studies to date have not assessed the contribution of single motor unit (SMU) action potentials to scalp recorded EEG. Furthermore, a study on the interference of SMU activity in relaxed position is necessary because the EEG signal is a clinical indicator of the cortical activity, such as coma state [95]. Various narrow-band frequency components are evaluated as cortical electrical oscillations, hence, the EMG activity emphasize an important problem.

CHAPTER 4

METHODS

4.1. Subjects

Data were collected from 9 healthy subjects (8 male, 1 female) (20-32 years). All volunteers gave written consent for the experimental procedures. The study was approved by the Koç University Local Ethics Committee. All subjects were right handed, none had temporomandibular joint disorder.

4.2. Experimental Setup

EEG activity was recorded with the 10-20 system EEG Headcap (MEDCAp, Spes Medica S.r.l, Italy) with 21 Ag/AgCl electrodes (Fig 4.1). The electrodes Fp1, Fp2, Fz, F3, F4, F7, F8, C3, C4, T3, T4, T5, T6, Pz, P3, P4, O1, O2, all referenced to Cz, were used. The clip electrode for grounding was attached to the right ear lobe and electrode impedances were kept below 20 kOhm by filling the electrode-tissue interface with conductive gel (ElectroGel) (Fig 4.1).

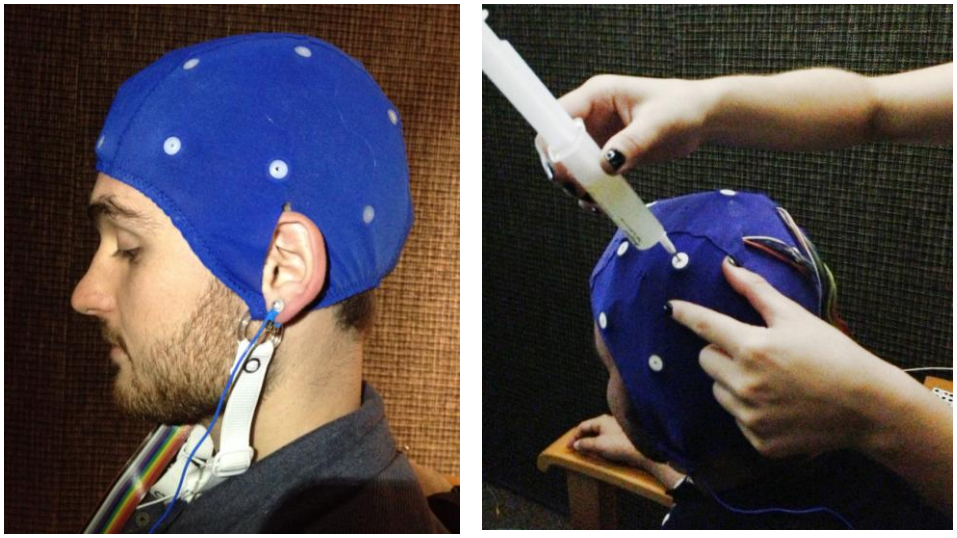

Fig. 4.1 :EEG preperation. Left figure shows the placement of the 10-20 system EEG Headcap. Right figure demonstrates the filling the electrode-tissue interface with conductive gel.

SMU activity was recorded with the two intramuscular silver fine-wire electrodes coated with Teflon (75 μm in core diameter) (MEDWIRE, USA) in Fig 4.2. The tips of the

wires were stripped off their Teflon coating about 3 mm to record the electrical activity of motor units from a bigger volume. The medial border of the left temporalis was detected by palpation while the subject was strongly biting (Fig 4.2). The 25G surgical needle with the pair of wires inside it was inserted in the 1-2 cm above of the midline of zygomatic arch into the relaxed muscle. The needle was immediately withdrawn leaving 'fish-hooked' electrodes within the muscle.

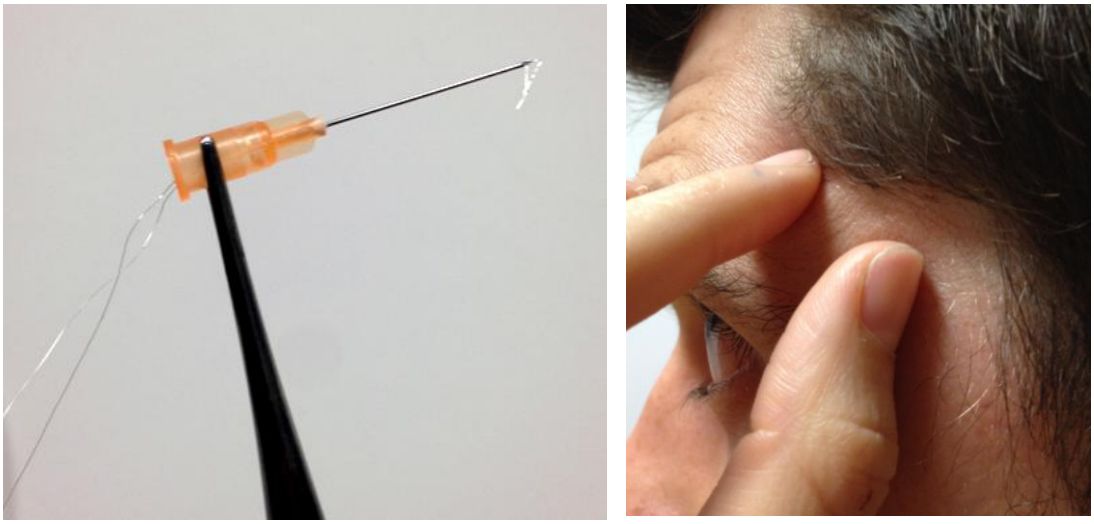

Fig 4.2 : Intramuscular electrodes. Left figure shows the SMU wire electrodes . Right figure demonstrates the palpation of the anterior temporalis

During recordings subjects were seated comfortably in an armchair inside an isolated EEG chamber with a Faraday Cage (Fig 4.3). They were instructed to relax unless asked by the experimenter to make specific facial movements. Their heads were unsupported. After placing the EEG cap and inserting the indwelling pair of wire electrodes, EEG and SMUs activity were recorded concurrently.

Fig. 4.3: Experimental EEG recording condition

The same SMUs were followed for 4-5 minutes in to have enough number of motor unit discharges for averaging purposes. A typical experiment with a specific SMU consisted of three EEG-SMU recording trials: eyes open, eyes closed, and dropped and relaxed jaw. The same procedure was followed for each SMU. The EEG epochs containing voluntary muscle contraction such as clenching the teeth, swallowing, shutting the eyes tight and raising the eyebrows were excluded from the data.

EEG-SMU data were collected with the same software (SystemPlus, Micromed S.p.A, Italy) and amplifier (Micromed S.p.A, Italy). The sampling rate was 4096 Hz, and filters were set to 0,15 Hz high pass and 1500 Hz low pass. A 100 Hz HP filter was applied to the EMG channel only for monitoring the unit potentials with ease during the experiment.

4.3. Analysis

The recorded SMU and EEG data were exported to Spike2 (Cambridge Electronic Design, England) for further analysis. SMU channels were high pass filtered with values between 60-100Hz. SMU decomposition analysis separated each action potential. Identified action potentials of SMUs were used as triggers and EEG signals as source in a spike triggered averaging (STA) procedure to assess the amount of EMG interference (Fig 4.4)

By taking SMU action potentials as triggers in the previously defined epochs, each EEG channel was averaged within ±50 ms around the triggers. The STA process resulted in different amplitudes of interference potentials, which were referred in this study as Macro-

EMEG (electro-myo-encephalogram). Cz-referenced potentials were converted into reference free Macro-EMEG by using Average Reference (AR) Method [62]. The calculated mean of all EEG channels was substracted from each channel.

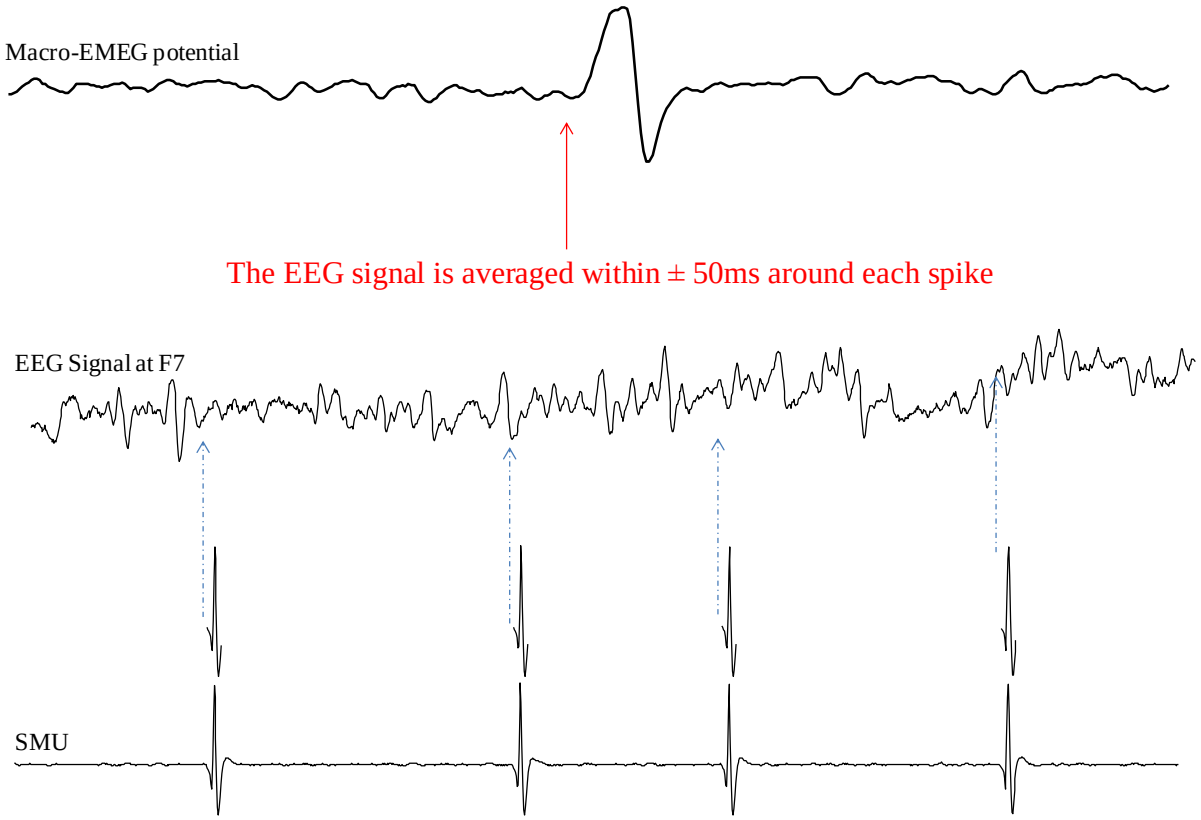

Fig 4.4: Detailed illustration of the spike triggered averaging of the EEG signal. By taking SMU action potentials as triggers in the previously defined epochs, each EEG channel was averaged within ±50 ms around the triggers. The STA process resulted in different amplitudes of interference potentials, which were referred in this study as Macro-EMEG (electro-myo-encephalogram).

Global field power (GFP, [96]) analysis determined the latency information of Macro-EMEG potentials. The GFP (1) calculates the root mean square amplitude deviations of all potentials within a field:

$$GFP = \sqrt{\sum_{i=1}^{N}\left(U_i - \frac{1}{n}\sum_{j=1}^{n} U_j\right)^2} \quad (1)$$

After calculation of the GFP values of each potential with the formula in (1), latency values were compared. Last step was the normalization of Macro-EMEGs as the percentage of the greatest Macro-EMEG amplitude to compare the spatial distribution.

CHAPTER 5

RESULTS

5.1. Analayzed SMUs

Seventeen different SMUs were identified from the 6 subjects in which we detected SMU activity. We could not record SMU activity from the 3 of 9 subjects. The same motor unit had multiple epochs of discharge during the recording. Each episode of continuous discharge was treated as a new SMU-train. Respectively, 39 SMU-trains were used as a trigger for the STA process (Table1). The mean discharge frequency was 15, 9 ± 3,6 Hz for all records. Thirty one SMU-trains belonging to 12 unique SMUs generated Macro-EMEG potentials and were used in further amplitude calculations (Table2).

Table 1. Condition and frequency information of SMUs. SMUs in left and middle columns generated prominent Macro-EMEGs, SMUs in right column were not represented in Macro-EMEG (EO: Eyes open, C: eyes closed, J: jaw dropped). Note that the discharge rates could be given only when there was a single motor unit activity during a predetermined condition. Therefore, jaw drop (J) condition, where most of the existing single unit activity stopped, was under represented in the Table.

SMU	Condition	Discharge Freq (Hz)
1	EO	16,8
	EO	15,5
	EO	13,3
2	EO	15,2
	C+J	12,6
	EO	14,4
3	EO	16,8
	C	15,3
	EO	16,2
4	EO	11,5
	EO	12,2
	EO	13,4
	EO+J	13,7
	C	13,4
5	EO	16,1
6	C	14,8

SMU	Condition	Discharge Freq (Hz)
7	EO	18,0
	C	16,0
8	EO	22,4
	EO	22,7
	EO	22,4
	C	20
	EO	22,1
9	C	11
	C	18,4
	EO	16,7
10	EO	18
	EO	11,9
	C	10,5
11	EO	17,6
12	EO	11,7

SMU	Condition	Discharge Freq (Hz)
1	EO	10,5
	EO	13,6
	EO	11,3
2	C	19,1
	C	22,7
3	EO	17
4	EO	17
5	EO	19,8

Table 2: Amplitude values of Macro-EMEGs for all SMUs (µV) (Tr.s: SMU-Trains, C:eyes closed, J: jaw dropped, others: eyes open)(empty cells: no prominent potential)

SMU	Tr.s	F7	FP1	F3	C3	T3	T5	P3	O1	FZ	CZ	PZ	FP2	F8	F4	C4	T4	T6	P4	O2
1	1	17,9	4,5	1,94	0,94	2,01	2,6	1,99	2,53	0,52	1,91	1,1		1,77	1,06	1,68	2,07	2,17	2,05	2,48
	2	11,9	1,7	1,18	0,43	0,71	1,46	1,15	1,42		1,12	0,87		1,14	0,82	1,08	1,47	1,39	1,32	1,53
	3	16,4	3,92	1,87	0,7	1,96	2,11	1,71	2,43		1,77	1,09		1,39	0,99	1,54	2,09	2,17	1,83	2,26
2	4	4,19	2,37	0,95	0,21	0,4	0,96	0,69	0,98		0,68	0,48	0,51		0,23	0,56	0,79	0,83	0,72	0,87
	5CJ	4,51	2,31	0,95		0,49	0,86	0,96	0,99			0,44	0,68		0,34	0,61	0,78	0,86	0,74	0,92
	6	3,18	2,2	0,81		0,63	0,8	0,52	0,9		0,54	0,34	0,59			0,55	0,52	0,78	0,65	0,95
3	7	7,36	4,25	2,46	0,63	2,05	1,63	1,17	1,76	0,36	1,06	0,77	0,38	0,8	0,55	0,93	1,06	1,2	1,08	1,35
	8C	6,85	4,15	2,52	0,48	1,3	1,36	1,09	1,44		1,07	0,72		1,18	0,69	1,02	1,23	1,22	1,15	1,21
	9	7,22	4,06	2,46	0,44	1,7	1,38	1,04	1,34	0,31	1,05	0,75	0,28	1,05	0,61	0,98	1,13	1,32	1,18	1,27
4	10	3,83	1,69	1,02			0,96	0,51	1,45		0,51		0,66							
	11	2,37	1,41	0,65			0,54		0,79		0,44	0,36	0,31			0,34		0,67	0,48	0,86
	12	2,35	1,13	0,46			0,45	0,35	0,55		0,34	0,27		0,29		0,3		0,56	0,32	0,68
	13J	2,07	1,18	0,62																
	14C	1	0,7	0,34		0,39	0,43	0,24				0,19								
5	15	3,75	0,74	0,62	0,16	0,74	0,55	0,39	0,67		0,44	0,27		0,37	0,25	0,42	0,53	0,61	0,52	0,68
6	16C	42,5	6,63	9	7,3	12,2	7,84	4,1	7,42	1,72	3,88	1,89		4,62	2,21	3,89	8,91	5,6	4,42	7,22
7	17	5,09	4,33	1,08			1,18	0,89	1,3		0,81	0,5	1,56			0,71		1,46	0,98	1,44
	18C	5,11	4,39	1,08	0,62	1,6	1,27	0,9	1,28			0,47	1,42							1,26
8	19	4,4	1,02	0,6			0,49	0,46	0,66		0,52	0,35	0,35	0,73		0,63	0,65	0,76	0,6	0,79
	20	3,84	0,92	0,44			0,52	0,49	0,54		0,71	0,43			0,51	0,44	0,46	0,65	0,81	0,64
	21	4,04	0,96	0,68			0,61	0,48	0,72		0,48	0,32		1,12				0,77	0,59	0,75
	22C	3,47	1,3					0,6	0,63		0,49	0,28				0,42		0,56		
	23	3,18	0,96	0,46					0,52			0,35				0,38	0,48		0,43	
9	24C	19,9	4,43	5,01	0,57	2,64	2,66	1,98	2,49		2,33	1,43	1,02	1,99	1,48	1,82	2,19	2,38	2,12	2,37
	25C	15,6	2,24	3,6		2,16	2,34	1,44	2,04		1,8	0,81	0,9	1,36	0,93	1,19	1,63	1,8	1,43	1,88
	26	20,8	3,85	4,69		2,06	2,58	1,98	2,55		2,31	1,41	1,1	2,05	1,39	1,81	2,45	2,5	2,1	2,46
10	27	9,19	9,42	2,75	0,69	2,41	2,78	1,82	2,07	0,62	2,05	1,13	0,98	0,92	0,51	1,27	0,5	1,97	1,67	2,09
	28	15,8	14,6	4,41	1,16	3,1	4,24	2,88	3,81	0,91	3,39	1,78	1,24	1,67	1	2,09	2,64	3,25	2,79	3,48
	29C	15,2	13,4	4,25	0,96	2,87	3,8	2,73	3,63	0,94	3,32	1,66	1,25	1,6	0,9	2,02	2,56	3,1	2,76	3,5
11	30	2,19	5,63	1,08	0,83	1,96	1,08	0,85	1,01	0,54	0,73	0,62	2,22		0,41	0,5	0,71	0,76	0,76	1,11
12	31	2,77	11,3	1,49	0,8	0,65			2,07	0,88	0,84	0,97	0,74	1,1	1,54	0,97	1,02	0,92	0,9	1,14

5.2. Location of the most prominent interference

When SMU spikes of temporalis muscle were used as the trigger for the STA process, SMUs generated prominent Macro-EMEG potentials on the ipsilateral-frontal and ipsilateral-parietal locations of the EEG. The F7 electrode was located just above the area where intramuscular electrodes recorded SMU potentials. (Fig 5.1.A). The Macro-EMEG potential of the F7 electrode was the most prominent and the greatest in amplitude amongst all the EEG channels for 10 SMUs (Fig 5.1.B) (Table2, F7 column).

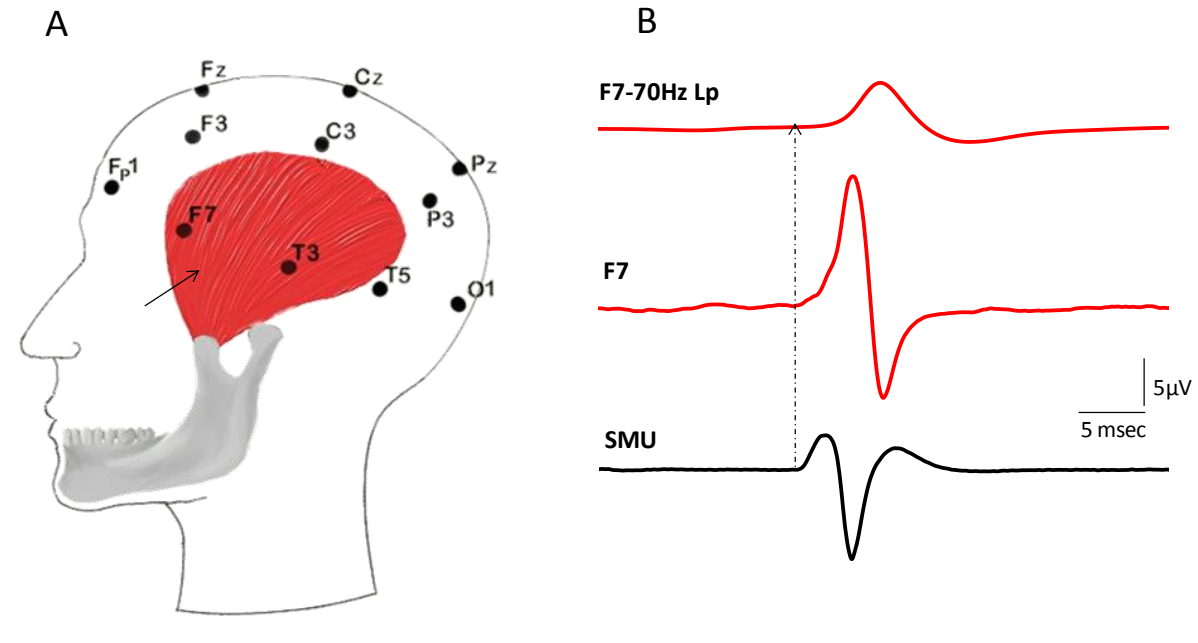

Fig. 5.1: Illustration of the locations of intramuscular electrodes, EEG electrodes, Macro-EMEG and SMU potential. ***A*** illustrates the locations of intramuscular electrode and ipsilateral EEG electrodes. Intramuscular wire is depicted as a black arrow placed on the anterior temporalis. ***B*** represents Macro-EMEG potentials from F7 channel with open filter (middle) and low pass filtered (top) using the motor unit action potentials recorded intramuscularly from the temporalis as trigger (bottom).

5.3. Topography of Macro-EMEGs

Temporalis activity in the rest condition contaminated the EEG at different scalp locations. Fig. 5.2.1, 5.2.2 and 5.2.3. demonstrate the widespread involvement of the resting muscle activity on the EEG signal for 12 SMUs. EEG records obtained from the electrodes closer to the SMU were contaminated the most by the SMU potentials. In particular, frontal electrodes F7, Fp1, F3 showed pronounced Macro-EMEG potentials indicating strong contribution of SMU activity on the EEG signal. Ten of 12 SMUs had the biggest Macro-EMEG at F7 and 2 SMUs at the Fp1 electrode. Contamination was not limited to frontal electrodes. Interference of one SMU was evident in other electrodes, which were fairly far from the SMU. However, for some electrode locations a clear potential was not observed after averaging. For example, the bottom figure (**C**) in Fig 5.2.1 shows non-prominent interference potentials in channels T5, P3 and A2. Nonetheless, the ipsilateral side of the head was found to be more susceptible to left temporalis activity compared to contralateral side in terms of the amplitude of the Macro-EMEG potentials. A clear phase reversal of the biphasic Macro-EMEG was observed across the coronal line. Polarity of the Macro-EMEGs changed due to the orientation of dipolar sources. Figures **C, E** and **L** show the polarity change between Fp1 and F7 while in other figures polarity was the same.

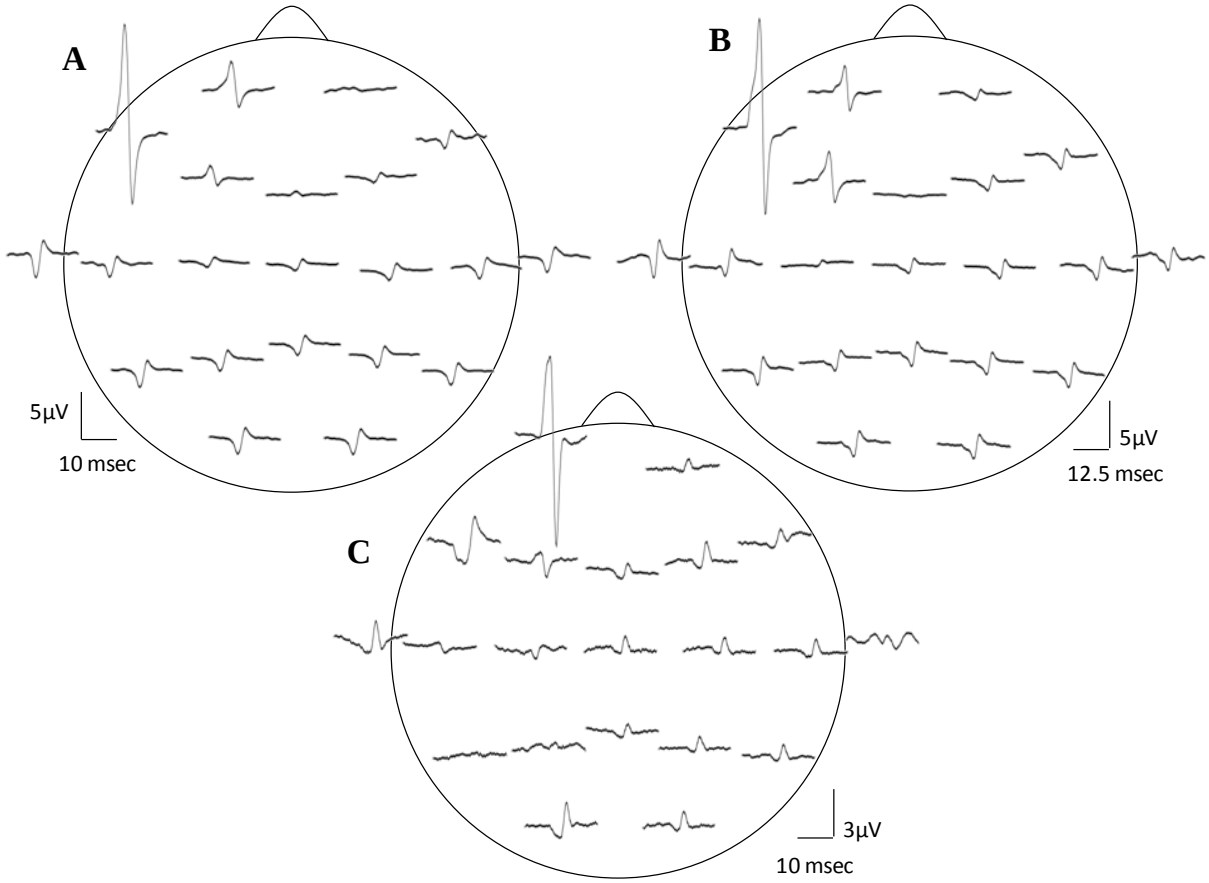

Fig. 5.2.1: Topography of the Macro-EMEG waveforms of 3 different SMUs (A, B, C). In **A** and **B**, F7 had the biggest Macro-EMEG while in **C** Fp1 was the greatest due to the muscle fiber orientation from which the SMU signal was recorded. For the 3 different representations, ipsilateral side of the head and temporalis region was more susceptible to left temporalis activity. Top figure represents the placement of electrodes.

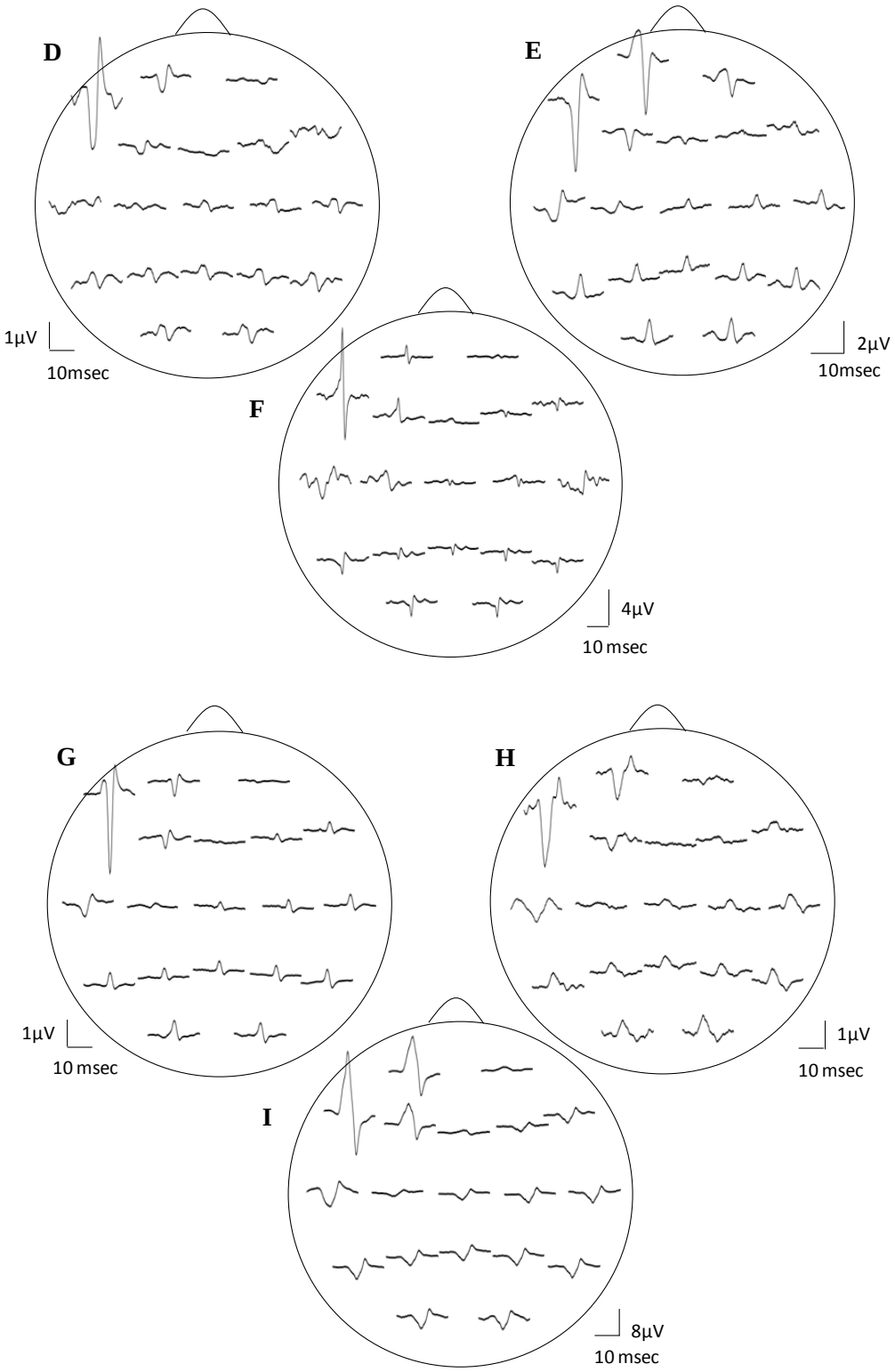

Fig 5.2.2: Topography of the Macro-EMEG waveforms of 6 different SMUs (D, E, F, G, H, I). In **ALL**, F7 had the biggest Macro-EMEG. **E** had high Fp1amplitude which is close to F7. For the 6 different representations, ipsilateral side of the head and temporalis region was more susceptible to left temporalis activity.

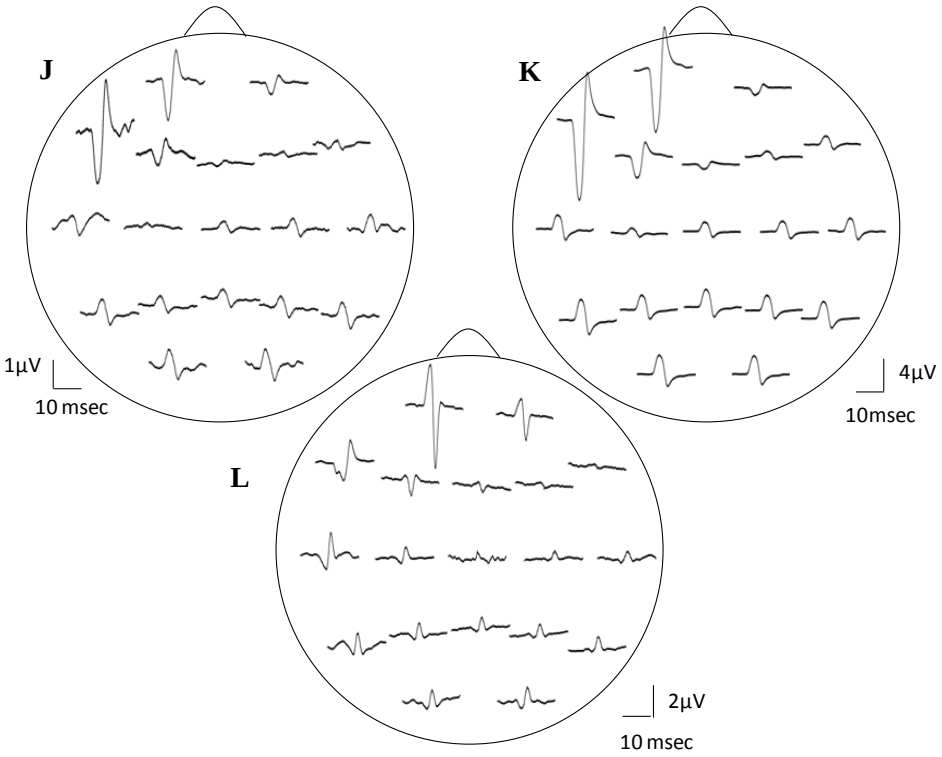

Fig 5.2.3: Topography of the Macro-EMEG waveforms of 3 different SMUs (J, K, L). In **J and K**, F7 had the biggest Macro-EMEG. **L** had the highest high amplitude at Fp1. For the 3 different representations, ipsilateral side of the head and temporalis region was more susceptible to left temporalis activity.

5.4. Timing of the Macro-EMEGs

Macro-EMEG potentials occurred synchronously over the skull. Fig 5.3 compares the global field power (GFP) with time course of the Macro-EMEG potentials recorded from the 21 electrodes. The left column shows the overlapping of Macro-EMEGs and GFP while the right column details the topography and phase reversal of Macro-EMEGs for the same SMU (Fig 5.3).There was no time delay between the occurrence of Macro-EMEG potentials indicating that the interference is a volume-conducting cross-talk event which does not involve neural conduction.

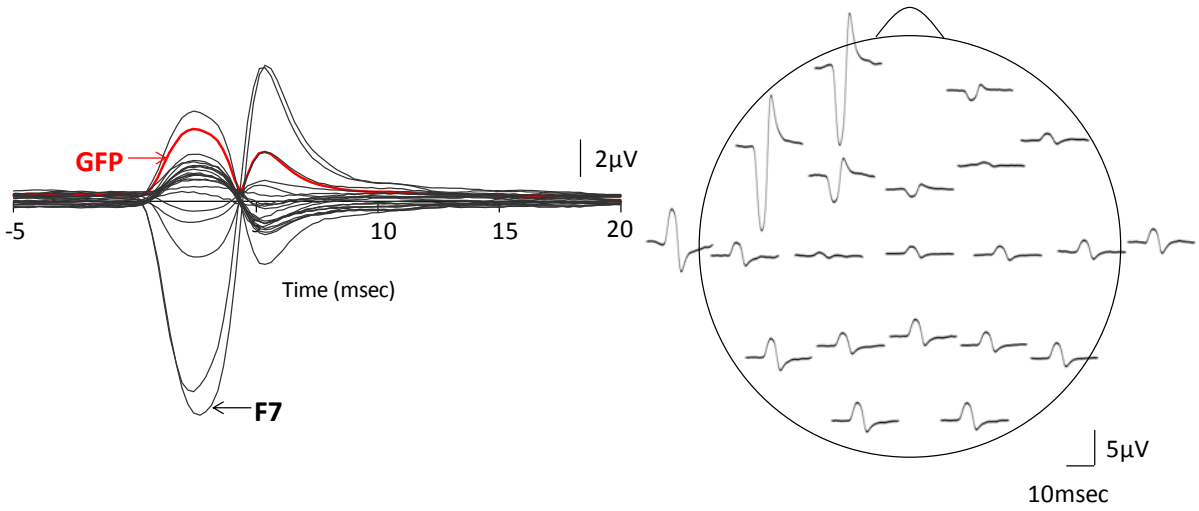

Fig. 5.3: Evidence fort he cross-talk. The left column presents the global field power versus time plot of the Macro-EMEG potentials from the 21 EEG electrodes and the right column shows the topography of Macro-EMEGs of the same SMU. Clear overlapping showsthe occurence of the potentials without a time delay. F7 had the greatest interference.

5.5. Visible SMU activity on the EEG signal

Discharging single motor units occurred in EEG channels simultaneously in the form of spikes (Fig 5.4). The temporalis SMU activity was the source of the spikes in F7 that appeared synchronously in Fig 5.4. T3 channel represented the activity of another active SMU. The contralateral side did not show SMU spikes for this particular epoch.

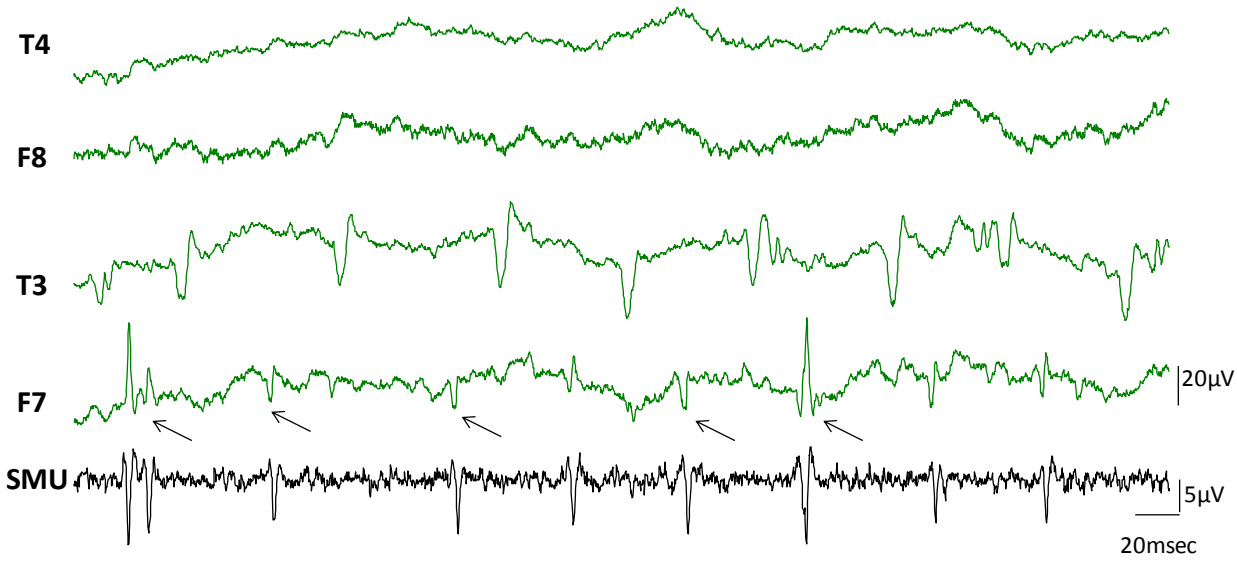

Fig 5.4: Visible SMU spikes in EEG records. SMU appeared on EEG channels during recording. Black arrows indicate the simultaneous spikes in SMU and F7. Spikes in T3 did not belong to the SMU followed.

5.6. Evaluation of Macro-EMEG contribution to EEG

Thirty one SMU-trains belonging to 12 SMUs produced Macro-EMEG potentials. Table 2 contains the amplitude values of SMU trains at each lead. Table 3 displays the contribution of the 29 SMU-trains as a percentage of F7 and 2 SMUs as a percentage of Fp1. To point out the differences in contribution of each motor unit, all channels were normalized to percentage of F7 for 29 SMU-Trains in Fig 5.5. Postural temporalis muscle activity affected frontal and temporal locations the most, particularly ipsilateral electrodes (Figure 5.5, top panel). Two SMUs which had the highest Macro-EMEG amplitude on Fp1 (Table 2, SMUs 11 and 12) were not included in Fig 5.5.

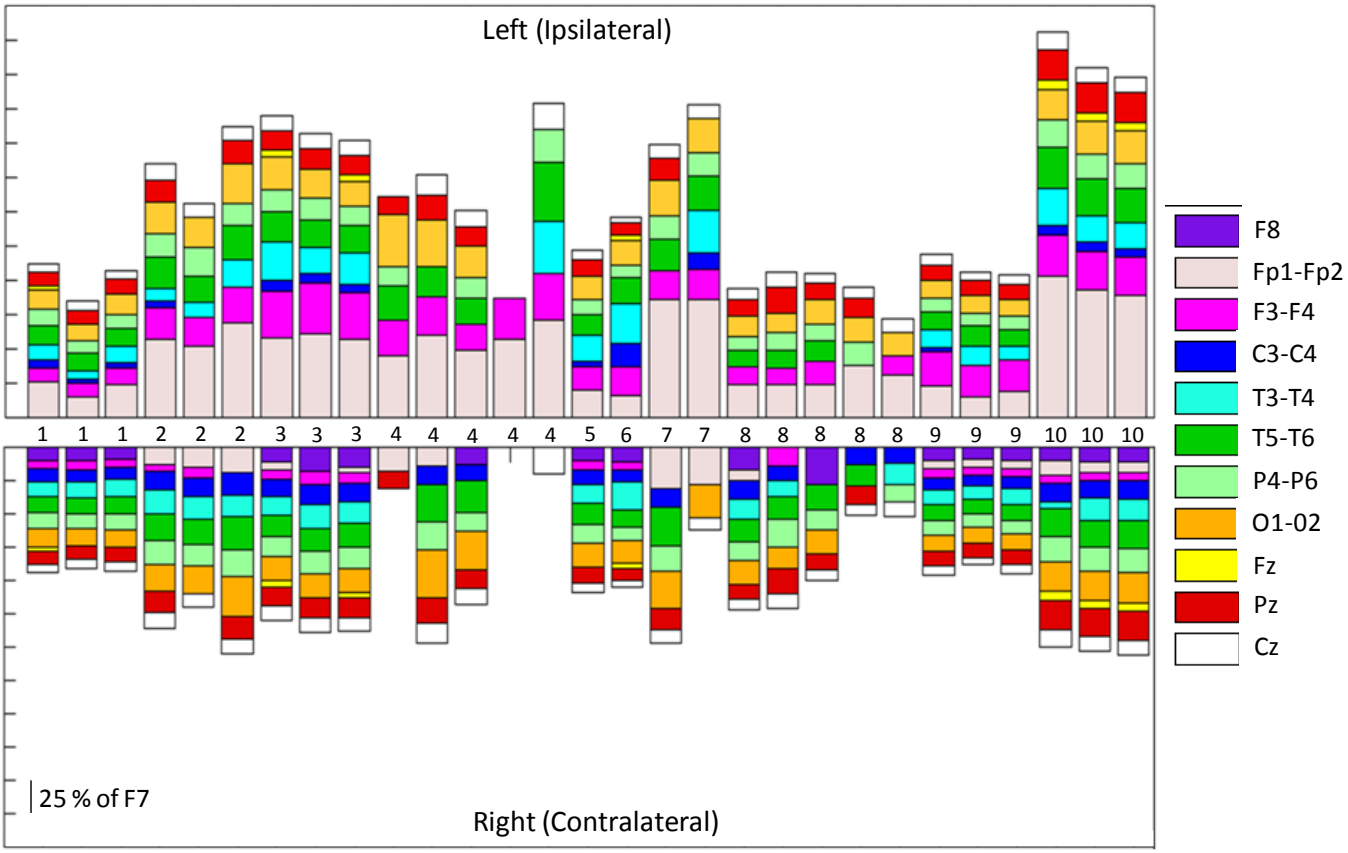

Fig 5.5: Relative sizes of the SMU representation on different EEG electrodes. Stacked bar representation of the percentage contribution of 29 SMU-trains to Left and Right Side EEG electrodes. Each of the 29 SMU trains is represented as a bar in horizontal axis. All Macro-EMEGs were normalized to F7 as 100 percent so F7 is not depicted.

Table 3: Percentage contribution of SMUs to EEG electrodes (%) (Tr.s: SMU-Trains, C:eyes closed, J: jaw dropped, others: eyes open)(empty cells: no prominent potential)

SMU	Tr.s	F7	FP1	F3	C3	T3	T5	P3	O1	FZ	CZ	PZ	FP2	F8	F4	C4	T4	T6	P4	O2
1	1	100	25,1	10,8	5,3	11,2	14,5	11,1	14,1	2,9	6,2	10,7	-	9,9	5,9	9,4	11,6	12,1	11,5	13,9
	2	100	14,3	9,9	3,6	6,0	12,3	9,6	12,0	-	7,3	9,5	-	9,6	6,9	9,1	12,4	11,7	11,1	12,8
	3	100	23,9	11,4	4,2	11,9	12,9	10,4	14,8	-	6,6	10,8	-	8,5	6,0	9,4	12,8	13,2	11,1	13,8
2	4	100	56,5	22,7	5,0	9,6	23,0	16,4	23,4	-	11,5	16,1	12,2	-	5,5	13,3	19,0	19,9	17,2	20,8
	5CJ	100	51,2	21,0	-	10,9	19,0	21,2	21,9	-	9,8	0,0	15,0	-	7,6	13,6	17,3	19,1	16,3	20,5
	6	100	69,0	25,5	-	19,8	25,2	16,4	28,4	-	10,8	17,0	18,4	-	-	17,4	16,2	24,6	20,3	29,8
3	7	100	57,8	33,5	8,5	27,9	22,1	15,9	24,0	4,8	10,4	14,4	5,2	10,9	7,4	12,6	14,4	16,3	14,6	18,3
	8C	100	60,5	36,8	7,0	19,0	19,8	15,9	21,1	-	10,4	15,7	-	17,2	10,1	14,9	17,9	17,8	16,8	17,7
	9	100	56,2	34,0	6,1	23,5	19,1	14,4	18,6	4,3	10,3	14,6	3,9	14,5	8,5	13,6	15,7	18,3	16,3	17,6
4	10	100	44,2	26,5	0,0	-	25,2	13,4	37,9	-	-	13,4	17,2	-	-	-	-	-	-	-
	11	100	59,4	27,6	-	-	22,9	0,0	33,2	-	15,1	18,7	13,1	-	-	14,3	-	28,4	20,3	36,5
	12	100	48,1	19,5	-	-	18,9	14,8	23,4	-	11,3	14,3	-	12,3	-	12,5	-	23,9	13,6	29,1
	13J	100	56,7	29,7	-	-	-	-	-	-	-	-	-	-	-	-	-	-	-	-
	14C	100	70,3	33,9	-	38,4	42,5	24,4	-	-	19,3	-	-	-	-	-	-	-	-	-
5	15	100	19,7	16,4	4,1	19,8	14,7	10,4	17,8	-	7,3	11,6	-	9,7	6,7	11,1	14,1	16,1	13,8	18,0
6	16C	100	15,6	21,2	17,2	28,7	18,4	9,6	17,5	4,0	4,4	9,1	-	10,9	5,2	9,2	20,9	13,2	10,4	17,0
7	17	100	85,1	21,2	-	-	23,2	17,5	25,6	-	9,8	16,0	30,7	-	-	13,9	-	28,6	19,3	28,3
	18C	100	86,0	21,2	12,0	31,3	24,8	17,6	25,1	-	9,1	-	27,7	-	-	-	-	-	0,0	24,7
8	19	100	23,1	13,7	-	-	11,2	10,5	15,1	-	8,0	11,7	7,8	16,5	-	14,2	14,7	17,3	13,7	17,9
	20	100	23,9	11,6	-	-	13,5	12,8	14,2	-	11,1	18,5	-	-	13,2	11,4	11,9	16,8	21,0	16,5
	21	100	23,7	16,9	-	-	15,1	11,8	17,7	-	7,9	11,9	-	27,7	-	-	-	19,0	14,6	18,6
	22C	100	37,4	-	-	-	-	17,4	18,0	-	7,9	14,0	-	-	-	12,1	-	16,1	-	-
	23	100	30,3	14,6	-	-	-	-	16,3	-	10,9	-	-	-	-	11,9	15,1	-	13,4	-
9	24C	100	22,2	25,1	2,9	13,3	13,4	9,9	12,5	-	7,2	11,7	5,1	10,0	7,4	9,2	11,0	11,9	10,6	11,9
	25C	100	14,3	23,0	-	13,8	15,0	9,2	13,0	-	5,2	11,5	5,8	8,7	6,0	7,6	10,4	11,5	9,1	12,0
	26	100	18,5	22,6	-	9,9	12,4	9,6	12,3	-	6,8	11,1	5,3	9,9	6,7	8,7	11,8	12,1	10,1	11,9
10	27	100	97,6	29,9	7,5	26,2	30,3	19,8	22,5	6,7	12,3	22,3	10,7	10,0	5,6	13,8	5,5	21,4	18,2	22,7
	28	100	92,2	27,9	7,3	19,6	26,7	18,2	24,0	5,7	11,3	21,4	7,8	10,5	6,3	13,2	16,7	20,5	17,6	21,9
	29C	100	88,4	28,0	6,3	18,9	25,0	18,0	23,9	6,2	10,9	21,8	8,3	10,5	5,9	13,3	16,9	20,4	18,2	23,1
11	30	38,8	100	19,2	14,7	34,8	19,1	15,2	18,0	9,5	10,9	13,0	39,4	-	7,3	8,9	12,6	13,5	13,5	19,8
12	31	24,5	100	13,2	7,1	5,8	-	-	18,3	7,8	8,6	7,4	6,5	9,8	13,6	8,6	9,1	8,2	7,9	10,1

5.7. Effect of closed eyes on the EMG interference

When subjects were instructed to close their eyes, some SMUs which were followed disappeared soon afterward. Nine of 17 SMUs continued firing after eye closing (Table1). Interference in eyes closed state was not different compared to the eyes open state. However, high frequency EMG activity on EEG signal, which was visible during recording, diminished in the eyes closed condition. Fig 5.6 compares two experimental conditions (eyes open and eyes closed) for visible SMU activity on EEG channels. Two different SMUs in Fig 5.6 generated similar Macro-EMEG amplitudes in both states (Table 3, SMU trains 7,8 and 17,18).

5.8. Effect of dropped-jaw on the EMG interference

Subjects also “dropped their jaws” to stop the temporalis from holding the mandible. Only 2 units (Table 3, trains 5,13) continued to fire after jaw dropping but other SMUs stopped firing. This observation suggests that the procedure may be useful for reducing the EMG interference of temporalis origin in EEG records.

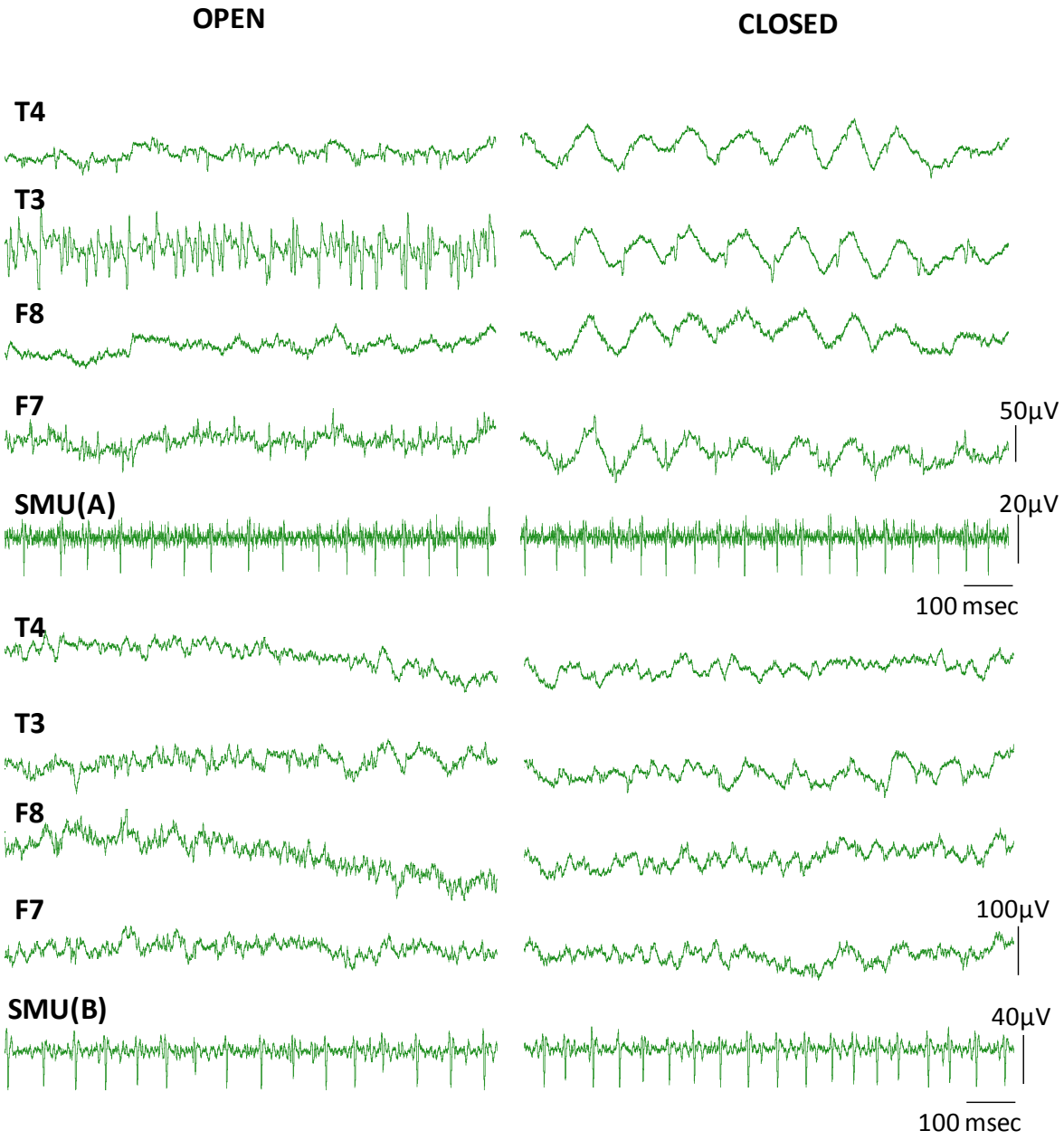

Fig 5.6: Effect of closing the eye. Comparison of visible EMG interference on EEG channels when eyes are open (left) and closed (right, grey column) in a relaxed sitting condition. Two different SMUs (top and bottom) continued discharging in eyes closed condition. EEG electrodes F7, F8 and T3, T4 were located on anterior and medial temporalis respectively**.**

CHAPTER 6

DISCUSSION

In this study we investigated the possible interference of the resting activity of muscles around the head on EEG records. We used the resting activity from the single motor units of the temporalis muscle as the trigger and averaged the simultaneously recorded electrical activity from the EEG electrode using a spike triggered averaging procedure. Seventeen different SMUs were identified from the 6 subjects in which we detected SMU activity. Respectively, 39 SMU-trains were used as a trigger for the STA process (Table1). Thirty one SMU-trains belonging to 12 unique SMUs generated Macro-EMEG potentials and were used in amplitude calculations and comparisons. The average potential was time-locked to the spike activity of the selected SMU. Our hypothesis stated that the resting SMU activity from the temporalis muscle contaminates the EEG records.

This study revealed the following original findings:

- Under 'rest' conditions, some activity of the muscles of the head continues, and contaminates EEG recordings even when no contamination was readily visible in the EEG channels.

- The contamination was location dependent and was most prominent on the side ipsilateral to the SMU recorded. However, interference was also notable in other electrodes that were further away from the site where SMU was recorded and even in the electrodes on the other side of the head.

- There was no time difference between the reflections of SMU on any pair of EEG electrodes indicating cross-talk.

- Eyes open and eyes closed conditions did not significantly alter the interference of SMU activity on the EEG records

- Jaw dropping activity stopped most of the active units and hence may be used as a routine procedure in the future EEG studies.

6.1. EMG activity at rest

In practice, rest position of a normal EEG study refers to a condition without any voluntary contraction of facial or masticatory muscles. Technologist should be aware of the subjects's conscious state to distinguish the abnormal EEG patterns and to maintain the resting conditions for silencing the visible EMG activity [60].

Formerly, the EEG recorded in rest was assumed to contain a very low level of EMG [25]. Furthermore, a widely accepted opinion supposes that the EEG is "EMG- free" in rest conditions [27, 44]. Goncharova and his colleagues (2003) revealed the presence of considerable interference from the pericranial muscles to the EEG in the experimental rest position [26]. Between successive voluntary contractions, measured activity of temporalis without contraction was assumed to be resting activity. The broad spectral peaks which were around 20 Hz and between 40-80 Hz in temporal areas during temporalis contraction attenuated in relaxation and all electrodes had a peak in the alpha range (about 10 Hz) in rest [26].

Accordingly, recent paralysis studies confirmed the EMG contamination of EEG [29, 49, 93]. Whitham et al., (2007) reported that the high frequency power which was quite evident around cranial and cervical muscles even in resting unparalysed state declined significantly after paralysis in the frequencies above 20-30 Hz [29]. Pope et al. (2009) showed a decrease in the "noisiness" of the EEG after muscle blockage [93]. The gamma power that was increasing with the mental task difficulty in un-paralyzed conditions was significantly lowered in paralyzed conditions especially around cranial muscles [51].

Aligned with previous findings, we demonstrated that some muscle activity continue around the head region under the 'rest' conditions and contaminate the EEG recordings. However, our approach to the monitoring of the EMG activity was critically different from previous studies. The continuous temporalis muscle activity was recorded via intramuscular wire electrodes.

6.2. SMU activity of temporalis

We recorded resting-intramuscular EMG activity of temporalis instead of surface EMG which was the common technique of previous EEG studies [24, 26, 27, 29, 39, 49]. The EEG montage itself or Ag/AgCl EMG electrodes were mostly placed on the muscle to detect the activity. It was shown that temporalis and frontalis muscles exhibits a low level of EMG activity even in the supine rest position [48]. Nonetheless, SEMG is susceptible to the crosstalk from the neighboring muscles [40].

Anatomically, the corrugator is located along the brow, orbicularis oculi turns around the eyes, frontalis rises above the brow, temporalis covers much of the temporal bone, masseter is placed on the jaw, the peri-auricular muscles surrounds the ear, and occipitalis covers the base of the skull. It is hardly possible to record the exact temporalis activity without recording frontalis or orbicularis oculi activity due to the anatomical proximity. Unlike surface electrodes, wire electrodes have selectivity. Consequently, we recorded SMU activity from the anterior part of temporalis (Fig 5.1-A) in physiological rest position of mandible which refers to a stable position of mandible relative to the maxilla (2-3 mm between the upper and lower incisors) [86]. Several intramuscular EMG studies revealed a specialized postural function for the anterior part [82- 85]. Blanksma and Van Eijden (1990) suggested that the anterior part performs continuous, low force activity while the posterior part is good at producing high force levels [82]. Of the 342 muscle spindles, 208 was found in the horizontal part of temporalis and 134 was in the vertical portion [90]. Dense spindle population of temporalis suggests the influence of proprioceptive mechanisms on the maintanence of mandibular posture. Therefore, type I fibers are dominant among type IIA, IIX and hybrids in temporalis. The dominance of type I fibers indicate its role in tonic activity since Type I fibers are activated first and the innervation ratio is small [91].

6.3. Location dependence of the interference

The contamination we observed was location dependent and was most prominent on the site of the muscle fiber involved. Fig 5.2 presents the topography of Macro EMEGs in which frontal F7 and Fp1 electrodes expressed the highest contamination. Because of the spatial orientations of the fibers from which we recorded SMU, polarity and amplitude of the most prominent Macro-EMEGs differed. Fig 6.1 shows the detailed orientations of fiber bundles and the direction of pull of the anterior fibers. Around the intramuscular electrode, the pull angle of fibers inclined anteriorly and declined medially [97].

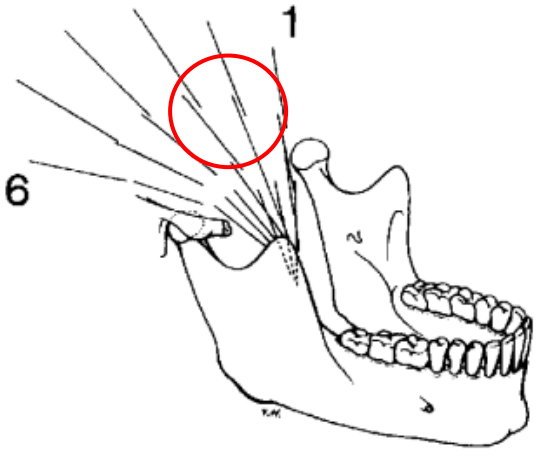

Fig 6.1: **Latero-cranio-anterior view of the temporalis fiber bundles at the closed jaw position**. The fiber bundles within each muscle portion have approximately the same orientation, except for those of the posteriormost portion, which are wrapped around the posterior root of the zygomatic arch.**1:** Anteriormost portion, **6:** posteriormost portion (Depicted from [97].Red circle shows the area of SMU recording.

Orientation of temporalis fibers evidences the clear phase reversal of the biphasic Macro-EMEGs when the average reference (AR) montage is preferred (Fig 5.2). Due to the "EEG reference problem" different reference choices may result in different Macro-EMEG topographies [62, 98, 99]. Referential montages had the possibility to make false localizations if an active reference is selected. The active reference is easy to recognize when the similar waveform appears in all the channels, especially in the proximity of the reference selected. When ipsilateral ear reference is used, temporal regions shows abnormal activities such as spikes or sharp waves. Therefore, for recording temporal abnormalities, Cz reference is widely used since Cz is far from the temporal lobes [60]. Since the average reference takes the voltages from all the locations and averages them to form a reference, the AR is successful for detecting focal abnormalities in any location if the reference is properly constructed by removing possible active and artifactual inputs [60]. However, the AR have the risk of being active if number of active electrodes are in included in the average [41]. In our study, we preferred the AR montage to demonstrate the interference of SMU on EEG. Therefore, spatial distribution of the EEG electrodes is limited to the upper surface of the head and ideal situation for AR is when electrodes cover evenly the whole surface of the head [99]. Fig 6.2 demonstrates the topographical difference between AR and right-ear (RE) reference. When the RE reference was applied, the Macro-EMEG amplitudes were even enhanced at frontal electrodes and they became smaller or even ceased at parietal and occipital electrodes because of the distance from the active electrodes of the left side. The observation that Macro-EMEG potentials were clearly pronounced on F7, F3 and Fp1 electrodes for both montages supports the hypothesis that interference from anterior temporalis is strongest around the muscle independently from the reference used.

The measure of global field power (GFP) shows the spatial standard deviation between the signals recorded from all electrodes. The maxima points of the GFP-time plots are compared to determine the latencies of the potentials [100]. This measure also illustrates the variation in the field strength over time. The GFP is not affected by the reference choice hence it is considered to be an independent descriptor of the potential field. In our calculations, the GFP resulted in no time delay (Fig 5.3); hence the reflections of SMU on EEG electrodes were synchronous, indicating cross-talk.

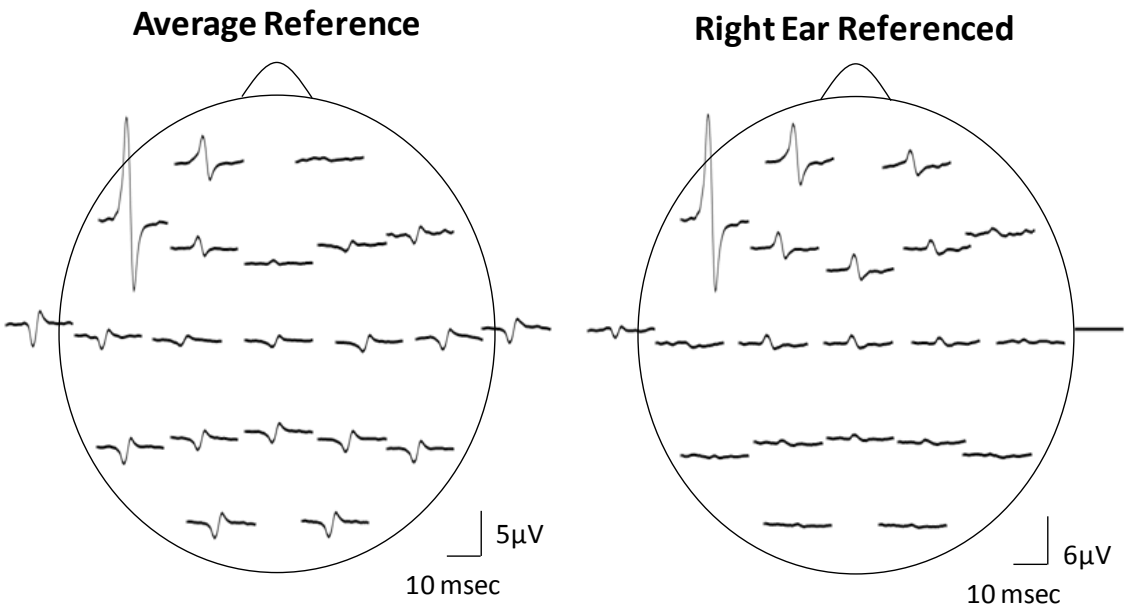

Fig 6.2: Effect of referencing. Comparison of AR and RE montages for the topography of Macro-EMEGs from 1 SMU. Amplitude and polarity of potentials differ between the two references. The RE reference emphasized the anterior temporalis location more than the AR in terms of the amplitude of Macro-EMEGs. This comparison also indicates the fact that the phase-reversal and amplitude enhancements seen with AR at parietal and occipital sites were not genuine but due to distortion of the scalp topography of potentials by the referencing method.

6.4. Magnitude of the EMG interference

The actual amplitude values of Macro-EMEG potentials varied slightly when measured in different episodes of the same SMU discharge because of the change in the impedance between the EEG electrodes and the reference electrode. However, variations even within the same SMU obstructed comparison of the distribution according to the measured amplitudes. Table 2 clearly shows the amplitude change within the same SMU. The magnitude of interference on each electrode location was compared by normalizing Macro-EMEG amplitudes to the percentage of the highest amplitude, either F7 or Fp1. After percentage normalization Macro-EMEGs showed similar percentage values for the same SMU. (Table3). Fig. 5.5 presents the magnitude of Macro-EMEG-potentials for different electrode locations. The SMU-trains belonging to same SMU had similar proportional distributions (Fig 5.5). The most dramatic difference was observed for the F7, Fp1, F3 and T3 due to the anatomical organization of temporalis fibers. However, artifactual components on

the inactive leads due to the active inputs of the potential fields remains as flaw of the AR method . Fig 5.5 also represents the contribution on the left and the posterior lead which are far from the SMU when the AR was preferred. Since these posterior potentials decrease significantly with the RE montage, they possibly represent the strong contribution of the F7, Fp1 and F3 to the average reference calculation.

6.5. Visible SMUs on EEG signal

During the recording we observed visually distinct, irregular and regular rhythmical spikes in the EEG epochs which disappeared and appeared occasionally. Spike pattern was similar to the previously described "common 'noise-like' pattern" "railroad cross-tie pattern" and "beta rhythm-like pattern" [26, 30].

In Fig 5.4 SMU activity of temporalis appeared on F7 channel synchronously, however, activity on the T3 channel originated from a different fiber, asynchronous to the SMU followed. Not only the ipsilateral side, also the contralateral side showed visible SMU activity in some subjects. Our observation of the visible SMU interference in rest emphasizes two important issues: comfort of the subject and the sampling regimen of the EEG signal. During recording, temporal, frontal, and occipital EEG channels reflected involuntary muscle activity, parallel to some observations reported [26, 30]. However, salient muscle activity was mostly diminished on the screen after conscious/intentional relaxation of subjects with an instruction. Consistent with our observation, it was suggested using stressful muscle regions as a biofeedback tool so that subjects can intentionally relax [30]. Moreover, alertness and stress caused by mental tasks given to subjects might cause a tension in facial muscles. When measured in the rest position, the EMG activity of frontalis, corrugators superciili [36, 53], and orbicularis oris inferior [36] increased with the increase in mental effort. Even tough we assumed that our subjects were in rest without voluntary contraction, it is not easy to eliminate the stress of experiment conditions on the subject. Likewise, the stress caused in the EEG clinics might be much more severe.

The interference from head muscles to the EEG is a critical point for the studies measuring cognitive function involving different mental tasks. Reliability of gamma band research is under discussion in terms of the contribution of scalp muscle activity. Several studies demonstrated that the EMG frequency spectra overlaps with the gamma band (30 Hz and above) [23, 93, 101, 102].Hence, it may be erronous to evaluate cognitive functions without considering the role of the EMG power.

In this study we showed that the term “rest” can be misleading because involuntary EMG activity from the temporalis continues in rest. A comprehensive investigation of SMU activity of facial muscles is an important need to evaluate muscle interference more reliably and to assess its possible effects on EEG more accurately. EMG interference may not be considered as an issue in ERP (event-related potential) studies because this technique is based on “event-time-locked” averaging of a fairly large number of EEG epochs. It should pose a serious problem, however, in ERO (event-related oscillation) research in which spectral components of “single” EEG sweeps or their average power spectra are evaluated but without any constraint of phase consistency.

Eyes open and closed positions did not significantly alter the interference of SMU activity on the EEG records. Nine of 17 SMUs continued firing after eye closing (Table1). A comparison of eyes open and eyes closed conditions did not reveal a consistent change in Macro-EMEG amplitudes. However, eyes affected the relaxation of subject and salient spikes on EEG channels were silenced remarkably after eye closing (Fig 5.6). When involuntary tension decreased by closing eyes, prominent SMU spikes also disappeared (Fig 5.6, SMU(A)). However, SMU (B) in Fig 5.6 continued discharging even the EEG trace showed no prominent spikes. This latter observation implies that “a clear EEG trace” does not necessarily rule out the existence of interference from the muscles around the head. We also observed that after subjects dropped their jaws, SMUs that were followed stopped firing in 1-2 seconds, so this instruction might be utilized in other EEG studies as an effort to minimize myogenic artifacts

6.6. Sampling of the EEG signal and important considerations

The sharp motor unit action potential contains high frequency components; therefore, the sampling rate for the SMU recording should be higher than 20 kHz [14]. Inadequate sampling of the high frequency SMU signal can distort the recorded data and the observed shape [14] . We recorded SMU activity with a sampling rate of 4096 Hz. The widest range of amplifier’s low-pass filter was instrumentally limited to 1500Hz which led to the skipping of high frequency-sharp motor units. In Fig 5.1.B, the duration of SMU (bottom trace) was about 10 msec. SMU spike waveform widened due to the low-pass effect of the system. Consequently, “the low pass effect” caused by the EEG/EMG recording system resulted in insufficient sampling of SMUs and artificially reduced the measured SMU amplitude contaminating the EEG. However, filters are usually set to 0.1 Hz high-pass and 35 Hz or 70

Hz low-pass [41] in routine clinical EEG. We observed that the clinically significant 70 Hz low-pass cannot prevent the interference of the SMU. Fig 6.3 shows that after 70 Hz low pass filtering the STA generated a prominent Macro-EMEG at F7 lead.

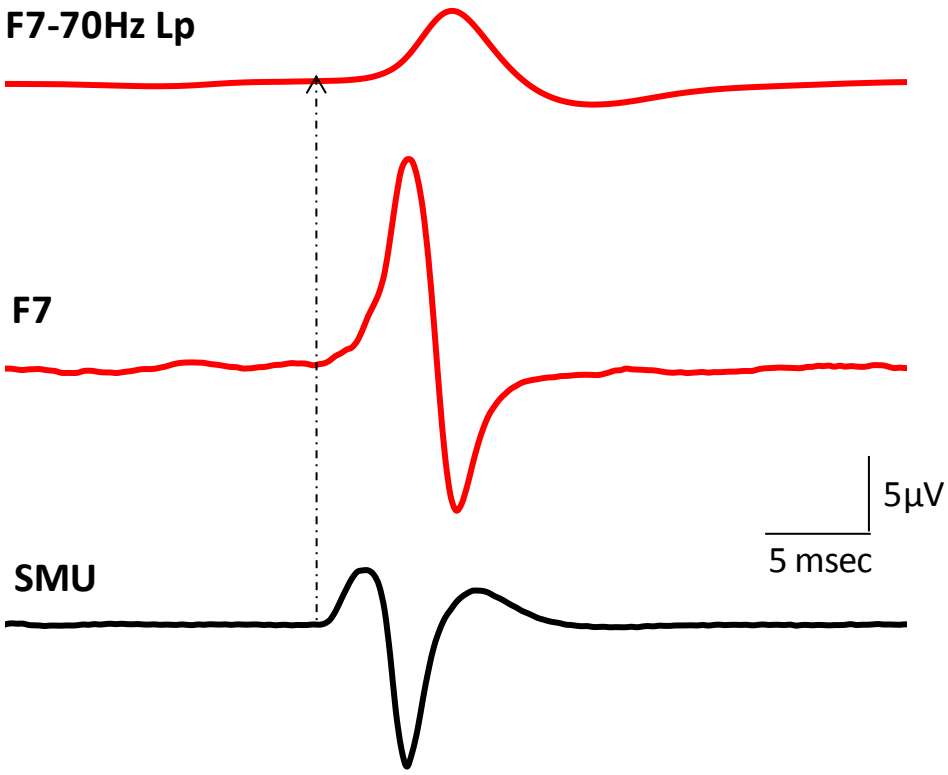

Fig. 6.3: Effect of filtering. Macro-EMEG at F7 lead without a low pass filter (middle trace) and with a 70 Hz low-pass (top trace) of the same SMU (bottom trace) in eyes open condition. Amplitude of the interference decreased and the timing was delayed due to low pass effect. However, potential was still visible and prominent. Averaging was depicted for ±50 msec

SMU activity during rest directly participated in the EEG signal (Fig 5.4, Fig 5.6) even when sampled with 4096 Hz. The majority of the studies investigated the EMG artifacts with an inadequate sampling rate (lower than 1000Hz) [25-27, 30, 39]. The "low-pass filtering" reduces the frequency content of SMU activity, hence making SMU activity look similar to the EEG waves. We strongly recommend using high sampling frequency for the recording and evaluation of the EEG signal, so that SMU activity will be sharply visible to recognize and to create algorithms to handle these artifacts.

CHAPTER 7

CONCLUSION

Our study examined the interference of the resting temporalis activity on the EEG records. The contamination was dependent on the location of the electrode relative to the muscle fiber SMU was recorded from and therefore was most prominent around the area of anterior temporalis. Both sides of the head were contaminated, but the ipsilateral side received stronger contamination. Even though we did not find a significant difference between the eyes open and closed positions regarding the interference from the SMUs, it was evident that other SMUs, which we did not follow, contributed to the EEG signal and were sometimes silenced in the eyes closed condition. Considering the results of study we suggest that recording of EEG should be made in eyes closed and jaw dropped position to decrease the amount of contamination from the resting activity of facial muscles. This measure is especially crucial in cases where "single" sweeps of EEG are analyzed and evaluated in time and frequency domains. This study might open a new path in evaluating the EMG contamination of the EEG and put further emphasis on the need for efficient artifact removal techniques. Starting point of our study, the question of " what makes the EEG" might be partially answered with the " brain activity together with the interfering muscle activity".

Bibliography

[1] Basmajian, J. V., De Luca C. J. (1985). "Introduction" in *Muscles Alive*, eds Basmajian, J. V. (Baltimore: Williams and Wilkins), 1-8.

[2] Collura, T. F. (1993). History and evolution of electroencephalographic instruments and techniques. *J. Clin. Neurophysiol*. 10, 476-504.

[3] Sanei, S., Chambers, J. A. (2007). "Introduction to EEG" in *EEG Signal Processing*. (West Sussex: John Wiley&Sons Ltd.), 1-30.

[4] Ungan, P., Yağcıoğlu, S. (2010). "Sources of the EEG and Brain's Evoked Potentials" in *Practical Guide on Electrodiagnosis*, eds Akyüz, G. (Ankara: Güneş Tıp Yayınevi), 379, 401.

[5] Speckmann, E. J., Elger, C.(1999). "Introduction to the neurophysiological basis of the EEG and DC potentials" in *Electroencephalography: basic principles, clinical applications, and related fields*, eds Niedermeyer, E., Lopes da Silva, F. (Philadelphia, PA: Lippincott Williams and Wilkins), 17-28.

[6] http://www.acm.org/conferences/sac/sac2000/Proceed/FinalPapers/BC-07/ Last Access: 22.07.14

[7] http://www.uthsc.edu/neuroscience/imaging-center/ Last Access: 22.07.14

[8] Kirschstein, T., Köhling, R. (2009). What is the source of the EEG?. *Clin. EEG Neurosci*. 40,146-149.

[9] Klass, D. (1995). The continuing challenge of artifacts in the EEG. *Am. J. EEG Technol.* 35, 239-269.

[10] Blount, J. P., Cormier, J., Kim, H., Kankirawatana, P., Riley, K. O., Knowlton, R. C. (2008). Advances in intracranial monitoring. *Neurosurg. Focus*. 25, E18.

[11] Arya, R., Mangano, F. T., Horn, P. S., Holland, K. D., Rose, D. F., Glauser, T. A. (2008). Adverse events related to extraoperative invasive EEG monitoring with subdural gridelectrod es: a systematic review and meta-analysis. *Epilepsia* 54, 828-839.

[12] de Luca, C. J., LeFever, R. S., McCue, M. P., Xenakis, A. P. (1982). Behaviour of human motor units in different muscles during linearly varying contractions. J. Physiol. 329, 113–128.

[13] Basmajian, J. V., De Luca C. J. (1985). "Description and analysis of the EMG signal" in *Muscles Alive*, eds Basmajian, J. V. (Baltimore: Williams and Wilkins), 65- 99.

[14] Türker, K. S. (1993). Electromyography: some methodological problems and issues. *Phys. Ther*. 73, 698–710.

[15] Loeb, G. E., Gans, C. (1986). "Single unit electromyography" in *Electromyography for Experimentalists* (Chicago, Ill: The University of Chicago Press), 292- 300.

[16] Fatourechi, M., Bashashati, A., Ward, R. K., Birch, G. E. (2007). EMG and EOG artifacts in brain computer interface systems: a survey. *Clin. Neurophysiol*. 118, 480–494.

[17] Nikamura, M., Shibasaki, H. (1987). Elimination of EKG artifacts from EEG records: a new method of non-cephalic referential EEG recording. *Electroenceph. Clin. Neurophysiol*. 66, 89-92.

[18] Jiang, J. A., Chao, C. F., Chiu, M. J., Lee, R. G., Tseng, C. L., Lin, R. (2007). An automatic analysis method for detecting and eliminating ECG artifacts in EEG. *Comput Biol. Med*. 37, 1660-1671.

[19] Sijbers, J., Audekerke, J. V., Verhoye, M., Van der Linden, A., Van Dyck, D. (2000). Reduction of ECG and gradient related artifacts in simultaneously recorded human EEG/MRI data. *Magn. Reson. Imaging.* 18, 881-886.

[20] Croft, R. J., Barry, R. J. (2000). Removal of ocular artifact from the EEG. *Neurophysiol. Clin*. 30, 5-19.

[21] Kong, W., Zhou, Z., Hu, S., Zhang, J., Babiloni, F., Dai, G. (2013). Automatic and direct identification of blink components froms EEG. *Sensors* 13, 10783-10801.

[22] Yuval-Greenberg, S., Tomer, O., Keren, A. S., Nelken, I., Deouell, L. Y. (2008). Transient induced gamma-band response in EEG as a manifestation of miniature saccades. *Neuron* 58, 429–441.

[23] Kovach, C. K., Tsuchiya, N., Kawasaki, H., Oya, H., Howard III, M. A., Adolphs, R. (2011). Manifestation of ocular-muscle EMG contamination in human intracranial recordings. *Neuroimage* 54, 213–233.

[24] O'Donnell, R. D., Berkhout, J., and Adey, W. R. (1974). Contamination of scalp EEG spectrum during contraction of cranio-facial muscles. *Electroenceph. Clin. Neurophysiol*. 37, 145–151.

[25] van de Velde, M., van Erp, G., Cluitmans, P. J. M. (1998). Detection of muscle artefact in the normal human awake EEG. *Electroenceph. Clin. Neurophysiol*. 107, 149–158.

[26] Goncharova, I. I., McFarland, D. J., Vaughan, T. M., and Wolpaw, J. R. (2003). EMG contamination of EEG: spectral and topographical characteristics. *Clin. Neurophysiol*. 114, 1580–1593.

[27] Fu, M. J., Dally, J. J., Çavuşoğlu, M. C. (2006). A detection scheme for frontalis and temporalis muscle EMG contamination of EEG data. *Conf. Proc. IEEE Eng.Med. Biol. Soc*. 1, 4514–4518.

[28] ter Meulen, B. C., Peters, E. W., Tavy, D. L., Mosch, A. (2006). Wiggling ears: an unusual EEG artifact caused by muscle activity. *Clin. Neurophysiol*. 117, 1403–1404.

[29] Whitham, E. M., Pope, K. J., Fitzgibbon, S. P., Lewis, T., Clark, C. R., Loveless, S., et al. (2007). Scalp electrical recording during paralysis: quantitative evidence that EEG frequencies above 20 Hz are contaminated by EMG. *Clin. Neurophysiol*. 118, 1877–1888.

[30] Ma, J., Tao, P., Bayram, S., and Svetnik, V. (2012). Muscle artifacts in multichannel EEG: characteristics and reduction. *Clin. Neurophysiol*. 123, 1676–1686.

[31] Kumar, S., Narayan, Y., Amell, T. (2003). Power spectra of sternocleidomastoids, splenius capitis, and upper trapezius in oblique exertions. *Spine J.* 3, 339–350.

[32] Siegmund, G. P., Blouin, J. S., Brault, J. R., Hedenstierna, S., Inglis, J. T. (2007). Electromyography of superficial and deep neck muscles during isometric, voluntary, and reflex contractions. *J. Biomech. Eng*. 129, 66–77.

[33] Møller, E. (1976). "Evidence that the rest position is subject to servo-control,"in Mastication, eds D. J. Anderson and B. Matthews (Bristol: John Wright & Sons), 72–80.

[34] Woda, A., Pionchon, P., and Palla, S. (2001). Regulation of mandibular postures: mechanisms and clinical implications. *Crit. Rev. Oral Biol. Med*. 12, 166–178.

[35] Sumitsuji, N. (1986). EMG activities of facial muscles in resting state. *Electromyogr. Clin. Neurophysiol*. 26, 555–556.

[36] Waterink, W., van Boxtel, A. (1994). Facial and jaw-elevator EMG activity in relation to changes in performance level during a sustained information processing task. *Biol. Psychol*. 37, 183–198.

[37] Dimberg, U., Thunberg, M., Elmehed, K. (2000). Unconscious facial reactions to emotional facial expressions. *Psychol. Sci*. 11, 86–89.

[38] Friedman, B. H., Thayer, J. F. (1991). Facial muscle activity and EEG recordings: redundancy analysis. *Electroencephalogr. Clin. Neurophysiol*. 79, 358–360.

[39] Yong, X., Ward, R. K., Birch, G. E. (2008). "Facial EMG contamination of EEG signals: characteristics and effects of spatial filtering," in Communications, Control And Signal Processing. International Symposium. 3rd ISCCSP (St Julians: IEEE), 729–734.

[40] Türker, K. S., Miles, T. S. (1990). Cross-talk from other muscles can contaminate EMG signals in reflex studies of the human leg. *Neurosci. Lett*. 111,164–169.

[41] Niedermeyer, E. (1999). "The normal EEG of the waking adult," in Electroencephalography: Basic Principles, Clinical Applications, and Related Fields, eds Niedermeyer, E. and Lopes da Silva, F. (Philadelphia, PA: Lippincott Williams and Wilkins), 149–173.

[42] van Albada, J. S., Robinson, P. A. (2013). Relationship between electroencephalographic spectral peaks across frequency bands. *Front. Hum. Neurosci.* 7, 56.

[43] Criswell, E. (2011). "The basics of surface electromyography" in Cram's Introduction to Surface Electromyography. (Jones and Bartlett Publishers), 35-65.

[44] Akay, M., Daubenspeck, J. A. (1999). Investigating the contamination of electroencephalograms by facial muscle electromyographic activity using matching pursuit. *Brain Lang*. 66, 184–200.

[45] Carl, C., Açık, A., König, P., Engel, A. K., Hipp, J. F. (2012). The saccadic spike artifact in MEG. *Neuroimage* 59, 1657–1667.

[46] McMenamin, B. W., Shackman, A. J., Greischar, L. L., Davidson, R. J. (2011). Electromyogenic artifacts and electroencephalographic inferences revisited. *Neuroimage*. 54, 4-9.

[47] Marieb, E. (2008). Essentials of Human Anatomy and Physiology, 9th edition.(San Francisco, CA: Pearson Education)

[48] Jensen, R., and Fuglsang-Frederiksen, A. (1994). Quantitative surface EMG of pericranial muscles. relation to age and sex in a general population. *Electroencephalogr. Clin. Neurophysiol*. 93, 175–183.

[49] Fitzgibbon, S. P., Lewis, T. W., Powers, D. M., Whitham, E. W., Willoughby, J. O., Pope, K. J. (2013). Surface laplacian of central scalp electrical signals is insensitive to muscle contamination. *IEEE Trans. Biomed. Eng*. 60, 4–9.

[50] Fries, P., Scheeringa, R., Oostenveld, R. (2009). Finding gamma. *Neuron* 58, 303-305.

[51] Whitham, E. M., Lewis, T., Pope, K. J., Fitzgibbon, S. P., Clark, C. R., Loveless, S., et al. (2008). Thinking activates EMG in scalp electrical recordings. *Clin.Neurophysiol*. 119, 1166–1175.

[52] Roesch, M., Olson, C. R. (2007). Neuronal activityr to anticipated reward in frontal cortex: Does it represent value or reflect motivation? *Ann. N.Y. Acad. Sci*. 1121, 431–446.

[53] Cohen, B. H., Davidson, R. J., Senulis, J. A., Saron, C. D., and Weisman, D. R. (1992). Muscle tension patterns during auditory attention. Biol. Psychol. 33, 133–156.

[54] ter Meulen, B. C., Peters, E. W., Tavy, D. L., and Mosch, A. (2006). Wiggling ears: an unusual EEG artifact caused by muscle activity. Clin. Neurophysiol. 117, 1403–1404.

[55] McFarland, D. J., McCane, L. M., David, S. V., and Wolpaw, J. R. (1997). Spatial filter selection for the EEG-based communication. *Electroencephalogr. Clin.Neurophysiol*. 103, 386–394.

[56] Boudet, S., Peyrodie, L., Forzy, G., Pinti, A., Toumi, H., and Gallois, P. (2012). Improvements of adaptive filtering by optimal projection to filter different arti- fact types on long duration EEG recordings. *Comput. Methods Programs Biomed*. 108, 234–249.

[57] Jung, T. P., Makeig, S., Humphries, C., Lee, T. W., McKeown, M. J., Iragui, V., et al. (2000). Removing electroencephalographic artifacts by blind source separation. *Psychophysiology* 37, 163–178.

[58] Olbrich, S., Jödicke, J., Sander, C., Himmerich, H., Hegerl, U. (2011). ICA-based muscle artefact correction of EEG data: what is muscle and what is brain? Comment on McMenamin, et al. *Neuroimage* 54, 1–3.

[59] De Clercq, W., Vergult, A., Vanrumste, B., van Paesschen, W., van Huffel, S. (2006). Canonical correlation analysis applied to remove muscle artifacts from the encephalogram. *IEEE Trans. Biomed. Eng*. 53, 2583–2587.

[60] Bearden, S. (2007). EEG reviewing/ recording strategy. Am. *J. END. Technol.* 47, 1-19.

[61] Nunez, P. L., and Srinivasan, R. (2006). *Electric Fields of the Brain: The Neurophysics of EEG*, 2nd Edn. (New York, NY: Oxford University Press)

[62] Dien, J. (1998). Issues in the application of the average reference: review, critiques and recommendations. *Behav. Res. Methods* 30, 34–43.

[63] Mehrkanoon, S., Moghavvemi, M.. Fariborzi, H. (2007). "Real time ocular and facial muscle artifacts removal from EEG signals using LMS adaptive algorithm" in International Conference on Intelligent and Advanced Systems, ICIAS. (Kuala Lumpur: IEEE), 1245 – 1250.

[64] Gasser, T., Schuller, J. C., Gasser, U. S. (2005). Correction of muscle artefacts in the EEG power spectrum. *Clin Neurophysiol.* 116, 2044-50.

[65] Srinivasan, R., Nunez, P. L., Silberstein, R. B. (1998). Spatial filtering and neocortical dynamics: estimates of EEG coherence. *IEEE Trans Biomed Eng*. 45, 814-26.

[66] Ushiyama, J. (2013). Resonance between cortex and muscle: A determinant of motor precision. *Clin. Neurophysiol*. 124, 5–7.

[67] Plankar, M., Brezan, S., Jerman, I. (2012). The principle of coherence in multi-level brain information processing. *Prog. Biophys. Mol. Biol*. 111, 8-29.

[68] Rosenberg, J. R., Amjad, A. M., Breeze, P., Brillinger, D. R., Halliday, D. M. (1989). The Fourier approach to the identification of functional coupling between neuronal spike trains. *Prog. Biophys. Molec. Biol*. 53, 1–31.

[69] Halliday, D. M., Conway, B. A., Farmer, S. F., Rosenberg, J. R. (1998). Using electroencephalography to study functional coupling between cortical activity and electromyograms during voluntary contractions in humans. *Neurosci. Lett*. 241, 5–8.

[70] Brown, P., Farmer, S. F., Halliday, D. M., Marsden, J., Rosenberg, J. R. (1999) Coherent cortical and muscle discharge in cortical myoclonus. *Brain* 122, 461–72.

[71] Makeig, S., Bell, A. J., Jung, T. P., Sejnowski, T. J. (1996). Independen component analysis of electroencephalographic data. *Advances in Neural Information Processing Systems* 145-151.

[72] Delorme, A., Sejnowski, T., Makeig, S. (2007). Enhanced detection of artifacts in EEG data using higher-order statistics and independent component analysis. *Neuroimage.* 34, 1443-1449.

[73] Lagerlund, T. D., Sharbrough, F.W., Busacker, N.E. (1997). Spatial filtering of multichannel electroencephalographic recordings through principal component analysis by singular value decomposition. *J. Clin. Neurophysiol*. 14, 73-82.

[74] Viola, F. C., Thorne, J., Edmonds, B., Schneider, T., Eichele, T., Debener, S. (2009). Semi-automatic identification of independent components representing EEG artifact. *Clin. Neurophysiol*. 120, 868-77.

[75] Gao, J., Yang, Y., Lin, P., Wang, P. (2010). "Online EMG artifacts removal from EEG based on blind source separation" in InternationalAsia Conferenceon Informaticsin Control, Automationand Robotics. (Wuhan, IEEE), 28-30.

[76] Sweeney, K. T., McLoone, S. F., Ward, T. E. (2013). The use of ensemble empirical mode decomposition with canonical correlation analysis as a novel artifact removal technique. *IEEE Trans. Biomed. Eng.* 60, 97-105.

[77] Safieddine, D., Kachenoura, A., Albera, L., Birot, G., Karfoul, A., et al. (2012). Removal of muscle artifact from EEG data: comparison between stochastic (ICA and CCA) and deterministic (EMD and wavelet-based) approaches. *J. on Advan. in Signal Proces*. 2012:127.

[78] Browne, M., Cutmore, T. H. R. (2002). Low-probability event-detection and separation via statistical wavelet thresholding: an application to psychophysiological denoising. *Clin. Neurophysiol.* 113, 1403–1411.

[79] Hannam, A. G., McMillan, A. S. (1994). Internal organization in the human jaw muscles. *Crit. Rev. Oral Biol. Med*. 5, 55–89.

[80] Koolstra, J. H. (2002). Dynamics of human masticatory system. *Crit. Rev. Oral Biol. Med*. 13, 366-376.

[81] Standring, S. (2008). *Gray's Anatomy: The Anatomical Basis of Clinical Practice, Expert Consult, 40th edition* (Churchill: Elsevier).

[82] Blanksma, N. G., van Eijden, T. M. (1990). Electromyographic heterogeneity in the human temporalis muscle. *J. Dent. Res*. 69, 1686–1690.

[83] Blanksma, N. G., van Eijden, T. M. (1995). Electromyographic heterogeneity in the human temporalis and masseter muscles during static biting, open/close excursions, and chewing. *J. Dent. Res*. 74, 1318–1327.

[84] Blanksma, N. G., van Eijden, T. M., van Ruijven, L. J., Weijs, W. A. (1997). Electromyographic heterogeneity in the human temporalis and masseter muscles during dynamic tasks guided by visual feedback. *J. Dent. Res.* 76, 542–551.

[85] McMillan, A. S. (1993). Task-related behavior of motor units in the human temporalis muscle. *Exp. Brain Res*. 94, 336–342.

[86] Nairn, R. I. (1976). "The concept of occlusal vertical dimension and its importance in clinical practice," in Mastication, eds D. J. Anderson and B. Matthews (Bristol: John Wright & Sons), 58–65.

[87] Gingerich, P. (1979). The human mandible: Lever, Link or Both?. *Am J Phys Anthropol.* 51, 135-137.

[88] Michelotti, A., Farella, M., Vollaro, S., and Martina, R. (1997). Mandibular rest position and electrical activity of the masticatory muscles. *J. Prosthet. Dent.* 78, 48–53.

[89] Rilo, B., Santana, U., Mora, M. I., Cadarso, C. M. (1976). Myoelectrical activity of clinical rest position and jaw muscle activity in young adults. *J. Oral Rehabil*. 24, 735–740.

[90] Kubota, K., Masegi, T. (1977). Muscle spindle supply to the human jaw muscle. *J. Dent. Res*. 56, 901–909.

[91] Korfage, J. A., van Eijden, T. M. (1999). Regional differences in fibre type composition in the human temporalis muscle. *J. Anat.* 194, 355–362.

[92] Henneman, E. G., Carpenter, D. O. (1965).Functional significance of cell size in spinal motoneurons. *J.Neurophysiol*. 28, 560-580.

[93] Pope, K. J., Fitzgibbon, S. P., Lewis, T. W., Whitham, E. M., Willoughby, J. O. (2009). Relation of gamma oscillations in scalp recordings to muscular activity. *Brain Topogr*. 22, 13–17.

[94] De Luca, J. C., Merletti, R. (1988). Surface myoelectric signal cross-talk among muscles of the leg. *Electroencep. Clin. Neurophysiol*. 69, 568-575.

[95] Sethi, N. K., Sethi, P. K., Torgovnick, J., Arsura, E., Schaul, N., Labar, D. (2008). EMG artifact in brain death electroencephalogram, is it a cry of "medullary death"?. *Clin. Neurol. Neurosurg*. 110, 729–731.

[96] Lehmann, D. (1987). "Principles of spatial analysis," in Methods of Analysis of Brain Electrical and Magnetic Signals, Handbook of Electroencephalography and Clinical Neurophysiology, eds A. S. Gevins and A. Reamond (Amsterdam: Elsevier), 309–354.

[97] van Eijden, T. M., Koolstra, J. H., Brugman, P. (1996). Three-dimensional structure of the human temporalis muscle. *Anat. Rec*. 246, 565–572.

[98] Hagemann, D., Naumann, E., and Thayer, J. F. (2001). The quest for the EEG reference revisited: a glance from brain asymmetry research. *Psychophysiology* 38, 847–857.

[99] Nunez, P. L., and Srinivasan, R. (2006). Electric Fields of the Brain: The Neurophysics of EEG, 2nd Edn. New York, NY: Oxford University Press.

[100] Skrandies, M. (1990). Global field power and topographic similarity. *Brain Topogr*. 3, 137-141.

[101] Michel, C. M., Murray, M. M. (2009). Discussing gamma. *Brain Topogr*. 22, 1–2.

[102] Nottage, J. F., Morrison, P. D., Williams, S. C., Ffytche, D. H. (2013). A novel method for reducing the effect of tonic muscle activity on the gamma band of the scalp EEG. *Brain Topogr*. 26, 50–61.